

QUANTUM MONTE CARLO METHODS FOR FERMIONIC SYSTEMS:
BEYOND THE FIXED-NODE APPROXIMATION

A THESIS SUBMITTED TO
THE GRADUATE SCHOOL OF NATURAL AND APPLIED SCIENCES
OF
MIDDLE EAST TECHNICAL UNIVERSITY

BY

NAZIM DUGAN

IN PARTIAL FULFILLMENT OF THE REQUIREMENTS
FOR
THE DEGREE OF DOCTOR OF PHILOSOPHY
IN
PHYSICS

AUGUST 2010

Approval of the thesis:

**QUANTUM MONTE CARLO METHODS FOR FERMIONIC SYSTEMS:
BEYOND THE FIXED-NODE APPROXIMATION**

submitted by **NAZIM DUGAN** in partial fulfillment of the requirements for the degree of
Doctor of Philosophy in Physics Department, Middle East Technical University by,

Prof. Dr. Canan Özgen
Dean, Graduate School of **Natural and Applied Sciences**

Prof. Dr. Sinan Bilikmen
Head of Department, **Physics**

Prof. Dr. Şakir Erkoç
Supervisor, **Physics Department, METU**

Examining Committee Members:

Prof. Dr. Bilal Tanatar
Physics Department, Bilkent University

Prof. Dr. Şakir Erkoç
Physics Department, METU

Prof. Dr. Ümit Kızıloğlu
Physics Department, METU

Prof. Dr. Ramazan Sever
Physics Department, METU

Assist. Prof. Dr. Hande Toffoli
Physics Department, METU

Date:

I hereby declare that all information in this document has been obtained and presented in accordance with academic rules and ethical conduct. I also declare that, as required by these rules and conduct, I have fully cited and referenced all material and results that are not original to this work.

Name, Last Name: NAZIM DUGAN

Signature :

ABSTRACT

QUANTUM MONTE CARLO METHODS FOR FERMIONIC SYSTEMS: BEYOND THE FIXED-NODE APPROXIMATION

Dugan, Nazım

Ph.D., Department of Physics

Supervisor : Prof. Dr. Şakir Erkoç

August 2010, 61 pages

Developments are made on the quantum Monte Carlo methods towards increasing the precision and the stability of the non fixed-node projector calculations of fermions. In the first part of the developments, the wavefunction correction scheme, which was developed to increase the precision of the diffusion Monte Carlo (DMC) method, is applied to non fixed-node DMC to increase the precision of such fermion calculations which do not have nodal error. The benchmark calculations indicate a significant decrease of statistical error due to the usage of the correction scheme in such non fixed-node calculations. The second part of the developments is about the modifications of the wavefunction correction scheme for having a stable non fixed-node DMC algorithm for fermions. The minus signed walkers of the non fixed-node calculations are avoided by these modifications in the developed stable algorithm. However, the accuracy of the method decreases, especially for larger systems, as a result of the discussed modifications to overcome the sign instability.

Keywords: electronic structure calculations, quantum Monte Carlo, fermions

ÖZ

FERMİYONİK SİSTEMLER İÇİN KUANTUM MONTE CARLO YÖNTEMLERİ: SABİT DÜĞÜM YAKINLAŞTIRMASI ÖTESİ

Dugan, Nazım

Doktora, Fizik Bölümü

Tez Yöneticisi : Prof. Dr. Şakir Erkoç

Ağustos 2010, 61 sayfa

Kuantum Monte Carlo yöntemleri alanında, sabit düğüm yakınlaştırması kullanmadan fermiyon hesabı yapan difüzyon Monte Carlo (DMC) yönteminin hassasiyet ve kararlılığını arttırıcı geliştirmeler yapıldı. Geliştirmelerin ilk bölümünde, difüzyon Monte Carlo yönteminin hassasiyetini arttırmak için geliştirilmiş olan dalga fonksiyonu düzeltme tekniği, sabit düğümsüz DMC yöntemine, hassasiyeti arttırma amacı ile uygulandı. Yapılan deneme hesaplarında, dalga fonksiyonu düzeltme tekniği kullanılması sonucu istatistiksel hatalarda büyük düşüşler olduğu görüldü. Geliştirmelerin ikinci bölümü, kararlı bir sabit düğümsüz DMC algoritması geliştirmek amacı ile, dalga fonksiyonu düzeltme tekniği üzerinde yapılan bir takım değişiklikler hakkındadır. Bu kararlı yöntemde, sabit düğümsüz hesaplarda oluşan eksi işaretli yürüyücüler (walkers), açıklanan değişiklikler sayesinde engellendi. Ancak, bu yöntemle elde edilen sonuçların doğruluğunun, özellikle büyük sistemlerde, eksi işaret kararsızlığını engellemek için yapılan değişiklikler yüzünden azaldığı sonucuna ulaşıldı.

Anahtar Kelimeler: elektronik yapı hesapları, kuantum Monte Carlo, fermiyonlar

To my love Nilay

ACKNOWLEDGMENTS

I would like to thank my Supervisor Şakir Erkoç for his endless support in my studies. He was more than a supervisor for me in the last five years. I would like to thank Dr. İnanç Kanık for his friendship and collaborations in this thesis work. This work would not be possible without his non stopping ideas. I would like to thank past and current graduate students of our group : Dr. Emre Taşçı, Dr. Barış Malcıoğlu, Dr. Rengin Peköz and Deniz Tekin for their firendships and collaborations. I wish success to all of them in their future academic life. I would like to thank the professors of METU Physics Department giving a special place to Hande Toffoli and Bayram Tekin for their supports in this thesis work. I would like to thank past and current graduate students Kıvanç Uyanık, Nader Ghazanfari, Çağrı Şişman and Çetin Şentürk for the discussions about all branches of physics and also for their friendships. I also thank my family and my love for supporting me in my personal life.

TABLE OF CONTENTS

ABSTRACT	iv
ÖZ	v
DEDICATION	vi
ACKNOWLEDGMENTS	vii
TABLE OF CONTENTS	viii
LIST OF TABLES	xi
LIST OF FIGURES	xii
CHAPTERS	
1 INTRODUCTION	1
1.1 Schrödinger Equation for Many Electron Systems	2
1.1.1 Expectation value of an observable	3
1.1.2 Variational principle	3
1.1.3 Indistinguishable particles and the antisymmetry condition	4
1.1.4 Spin and spatial parts of the wavefunction	5
1.1.5 Electronic structure problem	5
1.2 Quantum Monte Carlo	7
1.2.1 Statistical sampling and the Metropolis algorithm	8
1.2.2 Monte Carlo integration	9
1.2.3 Variational Monte Carlo	9
1.2.4 Diffusion process as random walk	11
1.2.5 Diffusion Monte Carlo	12
1.2.6 Importance sampling DMC	15
1.2.7 Fermion sign problem (FSP) in DMC	17

1.2.8	Fixed-node approximation	18
1.3	DMC Beyond the Fixed-node Approximation	19
1.3.1	Released-node technique	19
1.3.2	Plus minus cancellation methods	20
1.3.3	Correlated walk of opposite signed walkers	21
1.3.4	Non-symmetric guiding functions and the fermion Monte Carlo	22
1.3.5	Using permutation symemtry	22
1.3.6	Other Strategies towards the solution of FSP	23
1.4	Fermion Trial Wavefunctions	24
2	WAVEFUNCTION CORRECTION SCHEME FOR NON FIXED-NODE DMC	27
2.1	Wavefunction Correction Scheme	27
2.1.1	Vacuum branchings	29
2.1.2	Amplitude ratio parameter	29
2.1.3	Expectation value calculation	30
2.2	Usage of the Correction Scheme in Non Fixed-Node DMC	31
2.2.1	Algorithm details	32
2.2.2	Parameters	33
2.2.3	Statistical error analysis	35
2.2.4	Benchmark computations	35
2.2.5	Discussion about the benchmark calculation results	41
2.3	Stable Non Fixed-Node Algorithm Using Correction Scheme	43
2.3.1	Downwards shift of the trial wavefunction	43
2.3.2	Vacuum branchings at walker positions	44
2.3.3	Two permutation cells and two reference energies	46
2.3.4	Harmonic fermion calculations using the stable algorithm	47
3	CONCLUSIONS	50
	REFERENCES	52
	APPENDICES	

A	PROOF OF THE VARIATIONAL PRINCIPLE	57
	CURRICULUM VITAE	59

LIST OF TABLES

TABLES

Table 2.1 Correction scheme computation results for two harmonic fermions. d : space dimension, $\varepsilon_1, \varepsilon_2$: disturbance parameter values, E_c : calculated energy expectation value using the correction scheme, E_{GS} : true value of the fermionic ground state energy, E_T : trial wavefunction energy (all energies are given in dimensionless units), N_w : stabilized number of walkers from each sign, r_n : ratio of the trial wavefunction normalization to the number of walkers from each sign, r_t : ratio of the comparison case computation time to the correction scheme computation time. 37

LIST OF FIGURES

FIGURES

Figure 1.1 Illustration of the imaginary time evolution in DMC method. Adapted from the review article of Foulkes et al. [8].	14
Figure 2.1 Dashed Line: Trial wavefunction $\Psi_T(\mathbf{x})$, Solid Line: Ground state wavefunction $\Psi_{GS}(\mathbf{x})$, Dotted Line: Difference function $\Psi_{GS}(\mathbf{x}) - \Psi_T(\mathbf{x})$	28
Figure 2.2 Wavefunction plots for correction scheme DMC computation of the two harmonic fermions in 1D. TOP: Trial wavefunction. MIDDLE: Difference between the true fermionic ground state and the trial wavefunction. BOTTOM: Average walker distribution during the DMC computation.	38
Figure 2.3 Calculated energy expectation value versus normalization ratio parameter r_n for harmonic fermions in 1D.	39
Figure 2.4 He atom $1s2s\ ^3S$ state trial wavefunction (Eq. 2.11) cross section on $r_1 = 2\ r_2$ surface. Node crossing is seen at $r_2 = 0.5$ a.u.	40
Figure 2.5 Downwards shift of the trial wavefunction $\Psi_T(\mathbf{x})$. Dashed Line: Shifted trial wavefunction $\Psi_T^s(\mathbf{x})$, Solid Line: Ground state wavefunction $\Psi_{GS}(\mathbf{x})$, Dotted Line: Difference function $\Psi_{GS}(\mathbf{x}) - \Psi_T^s(\mathbf{x})$	43
Figure 2.6 Position dependent shift of the trial wavefunction. Dashed Line: Shifted trial wavefunction $\Psi_T^s(\mathbf{x})$, Solid Line: Ground state wavefunction $\Psi_{GS}(\mathbf{x})$	44
Figure 2.7 Wavefunction plots for two harmonic fermions in 1D. Horizontal axes x_1, x_2 are the positions of the two fermions. TOP: Difference between the true fermionic ground state and the shifted trial wavefunction ($\Phi = \Psi_{GS} - \Psi_T^s$). BOTTOM: Average walker distribution during the DMC computation (D_w).	48

CHAPTER 1

INTRODUCTION

Finding the solution of the Schrödinger equation for a physical system is the first step for investigating various properties of the ground state or any excited states of the system. Current computational investigations in the nanoscience field demand accurate and large scale applicable techniques for finding especially the ground state solution of the Schrödinger equation for fermion systems. These mentioned two properties, high accuracy and large scale applicability, are the two major tradeoffs for the electronic structure calculation methods. There are highly accurate quantum chemistry methods [1, 2] lacking the large scale applicability property beside linear scaling methods [3, 4] applicable to very large systems which are not very accurate and not applicable to all kinds of systems. Density functional theory (DFT) [5, 6] is popular in this field because of its balance between the accuracy and the applicability. However, its accuracy is not enough for some systems where electron - electron correlation is significant.

Quantum Monte Carlo (QMC) methods [7, 8] provide more accurate results for such solutions of the Schrödinger equation and their application range is similar to DFT calculations. QMC methods are not as popular as DFT since their usage are not as straightforward. They require preliminary Hartree-Fock [9] or DFT calculations for trial wavefunction generation which is essential for both the *variational* and the *projector* Monte Carlo. The approximate *nodal hypersurface* of the trial wavefunction is used in the projector methods for the imposition of the antisymmetry condition of the fermionic wavefunction. This technique which is called as the fixed-node approximation [10] is currently a standard tool used in the projector QMC calculations. Techniques for the imposition of the antisymmetry condition without using the fixed-node approximation are being developed for many years and they are also the subject of this thesis work. However, application of these exact methods are limited to systems having

a few electrons because of the so called *fermion sign problem* arising from the antisymmetry condition of the fermionic wavefunction.

Origin of the fermion sign problem will be discussed in the subsequent sections after an introductory information is given about the Schrödinger equation, statistical sampling techniques and the QMC methods. The discussion in this thesis work is about the solutions of the time independent Schrödinger equation to find the energy eigenvalues of the lowest lying anti-symmetric eigenstates of nanoscale systems. The developments can be easily extended to calculate expectation values other than the energy. However, extensions towards studying the excited states or time-dependent solutions are not straightforward and they are not the subject of this thesis work. A basic quantum mechanics knowledge with Dirac's bracket notation [11, 12] is assumed throughout the discussion.

1.1 Schrödinger Equation for Many Electron Systems

Nonrelativistics physics is described by the Schrödinger equation [13] in the atomic and molecular scale. The evolution of the quantum mechanical wavefunction $\Psi(\mathbf{x})$ is governed by this complex wave equation:

$$i\hbar \partial_t \Psi(\mathbf{x}, t) = -\frac{\hbar^2}{2m} \nabla^2 \Psi(\mathbf{x}, t) + V(\mathbf{x}) \Psi(\mathbf{x}, t) \Psi_{GS}, \quad (1.1)$$

where \mathbf{x} is a vector in the configuration space spanned by the system variables (individual particle coordinates for the position space wavefunction) and $V(\mathbf{x})$ is the physical potential defining the system. The Planck's constant \hbar and the electron mass m (also the electron charge e) will not shown in the equations hereafter since they have the numerical value of 1.0 when the atomic unit system [6] is used. The static wave solutions of the above equation in which the physical system can be found are called as the *eigenstates* $[\Phi_i(\mathbf{x})]$ of the system. An energy *eigenvalue* (E_i) is defined for the all eigenstates according to the eigenvalue equation which is also called as the time independent Schrödinger equation:

$$\hat{H} \Phi_i(\mathbf{x}) = E_i \Phi_i(\mathbf{x}), \quad (1.2)$$

where \hat{H} is the Hamiltonian of the system. According to the Copenhagen interpretation [14,

15] of the quantum theory, the magnitude square of the complex wavefunction $\Psi(\mathbf{x})$ gives the probability distribution of the possible outcomes of the measurement process.

1.1.1 Expectation value of an observable

Quantum mechanics suggest that the outcome of a measurement process cannot be certainly known before the measurement when the system is in any state with wavefunction $\Psi(\mathbf{x})$. However, as stated in the previous subsection, the wavefunction can be used to calculate the probabilities of the outcomes. The most probable outcome of an observable \hat{O} can be calculated by the expectation value calculation as:

$$\langle \hat{O} \rangle = \frac{\langle \Psi(\mathbf{x}) | \hat{O} | \Psi(\mathbf{x}) \rangle}{\langle \Psi(\mathbf{x}) | \Psi(\mathbf{x}) \rangle} = \frac{\int \Psi^*(\mathbf{x}) \hat{O} \Psi(\mathbf{x}) d\mathbf{x}}{\int \Psi^*(\mathbf{x}) \Psi(\mathbf{x}) d\mathbf{x}} . \quad (1.3)$$

The integrals in the above equation are over the range of the vector \mathbf{x} and $\Psi^*(\mathbf{x})$ is the complex conjugate of the wavefunction $\Psi(\mathbf{x})$. The denominator of the expectation value expression is unity if the wavefunction $\Psi(\mathbf{x})$ is normalized. When the Hamiltonian \hat{H} of the system is taken as the observable, the energy expectation value of the quantum state is calculated using Eq. 1.3. The expectation value may be calculated for states which are not eigenstates of the observable \hat{O} . The observables of the quantum mechanics are represented by linear Hermitian operators and consequently the calculated expectation values and the eigenvalues are real.

1.1.2 Variational principle

Eigenvalues a_i of the Hamiltonian operator and many other observables are real numbers, one of them, the ground state eigenvalue a_0 having the lowest value:

$$a_0 < a_1 < a_2 < a_3 \dots \quad (1.4)$$

The variational principle states that the expectation value of an observable \hat{O} is always greater than or equal to a_0 if Eq. 1.4 holds:

$$\langle \hat{O} \rangle = \frac{\langle \Psi(\mathbf{x}) | \hat{O} | \Psi(\mathbf{x}) \rangle}{\langle \Psi(\mathbf{x}) | \Psi(\mathbf{x}) \rangle} \geq a_0 . \quad (1.5)$$

The proof of the above expression, which is given in Appendix A, uses eigenfunction decomposition of the arbitrary state $\Psi(\mathbf{x})$.

Variational principle is the basis for variational methods in which the ground state of the system is found by minimizing the expectation value of an observable which is most of the time the Hamiltonian of the system. The variational Monte Carlo method, discussed in Section 1.2.3, is such a variational method.

1.1.3 Indistinguishable particles and the antisymmetry condition

Quantum mechanical systems are composed of indistinguishable particles such as electrons. Indistinguishability states that the probability distribution (the magnitude square of the wavefunction) should be conserved under any particle permutations. As a consequence, the physical system is not affected from the exchange of any two quantum particles of the same kind:

$$|\Psi(\mathbf{x}_1, \mathbf{x}_2, \mathbf{x}_3, \dots, \mathbf{x}_n)|^2 = |\Psi(\mathbf{x}_2, \mathbf{x}_1, \mathbf{x}_3, \dots, \mathbf{x}_n)|^2, \quad (1.6)$$

where \mathbf{x}_n denotes the individual particle coordinates. The indistinguishability property results in two alternatives for the behavior of the wavefunction $\Psi(\mathbf{x})$ under particle exchanges. The wavefunction should either be totally conserved or it should be conserved with a change of sign when any odd numbered indistinguishable particle permutations occur. This symmetry of nature groups the elementary particles as bosons and fermions, bosons having conserved (symmetric) wavefunctions and fermions having sign alternating (antisymmetric) wavefunctions under the particle exchanges. The wavefunction being symmetric or antisymmetric determines the statistics of the quantum particles: Bosons obey Bose-Einstein statistics and fermions obey Fermi-Dirac statistics [16]. The Pauli exclusion principle which forbids any two identical fermions sharing a quantum state is actually a result of the antisymmetry condition of the fermionic wavefunction. The connection of these dissociated statistics with particle spins (discussed in next subsection) is established in the relativistic quantum theory [17].

Eigenstate spectrum of the Schrödinger equation for a specific system covers the all symmetric and antisymmetric solutions. The ground state solution with the lowest eigenvalue is always symmetric under particle permutations and therefore it can be occupied by bosons only. If the particles in the system are fermions such as electrons, the antisymmetric ground state of the

system is actually an excited state when the all possible static solutions are considered. This fact causes a challenge for the projector QMC methods which will be discussed in Section 1.2.7.

1.1.4 Spin and spatial parts of the wavefunction

Elementary particles have an extra degree of freedom in addition to the usual spatial degrees of freedom. This intrinsic property is called as spin [18] since it has the unit of angular momentum. The bosons and fermions discussed in the previous subsection differ also about the spin issue, former having integer spin values (0, 1 ...) and latter having half integer spin values (1/2, 3/2 ...).

The fermionic wavefunction, for which the antisymmetry condition holds, should involve the spin variables as well. Spin part of the wavefunction may be symmetric or antisymmetric under the particle exchanges and the spatial part should be the inverse in order to have an antisymmetric function in total. The spin and the spatial parts of the wavefunction may be inseparable in some cases for which the antisymmetry condition of the total wavefunction is the only criterion.

1.1.5 Electronic structure problem

Solving the time independent Schrödinger equation (Eq. 1.2) for a many electron system is called in the literature as the electronic structure problem. Ground state or any excited state, eigenvalue and eigenvector are obtained from the solution of Eq. 1.2. In the scope of this thesis work, ground state solutions for fermion systems are studied which are indeed excited states when the all possible solutions are considered as mentioned in Section 1.1.3.

The Hamiltonian function for a molecular system is composed of many terms:

$$\hat{H} = - \sum_k \frac{1}{2M_k} \nabla_k^2 - \sum_i \frac{1}{2} \nabla_i^2 + \sum_{k_1 k_2} \frac{Z_{k_1} Z_{k_2}}{|\mathbf{R}_{k_1} - \mathbf{R}_{k_2}|} + \sum_{i_1 i_2} \frac{1}{|\mathbf{r}_{i_1} - \mathbf{r}_{i_2}|} - \sum_{i k} \frac{Z_k}{|\mathbf{R}_k - \mathbf{r}_i|} . \quad (1.7)$$

The index k is over the all nuclei and the index i is over the all electrons in the all terms of the above expression. The first two terms are the kinetic energy terms of the nuclei and

the electrons respectively. The third term is the nucleus - nucleus potential energy term due to the Coulomb interaction between the nuclei where Z_k denote the nuclear charges and \mathbf{R}_k denote the position vectors of the nuclei. The fourth term is the equivalent potential energy term for the Coulomb interaction between the electrons, \mathbf{r}_i being the position vectors of the electrons. The last term is the potential energy term for the electron - nucleus interactions. The summations in the all potential energy terms go over the all corresponding particle pairs included in each term.

The above expression for the Hamiltonian should be substituted in Eq. 1.2 to find the solution for the desired state. However, the exact solution of the electronic structure problem can be found only for a few simple systems such as the hydrogen atom which has only one electron and one nucleus. Therefore, some approximations should be made to reduce the complexity of the problem.

The Born-Oppenheimer approximation [19] simplifies the Hamiltonian expression given in Eq. 1.7 using the fact that the nuclear motions are very slow compared to the electron motions. The nuclear motions are totally ignored in this approximation without losing much from the accuracy for most of the condensed matter systems. The first term of Eq. 1.7 vanishes in such a case and the third term becomes constant which can also be taken out in the solution process. The Hamiltonian with such reductions is called as the electronic Hamiltonian:

$$\hat{H}_e = - \sum_i \frac{1}{2} \nabla_i^2 + \sum_{i_1 i_2} \frac{1}{|\mathbf{r}_{i_1} - \mathbf{r}_{i_2}|} - \sum_{i k} \frac{Z_k}{|\mathbf{R}_k - \mathbf{r}_i|}, \quad (1.8)$$

for which the nuclear positions \mathbf{R}_k are included as parameters in the last term which is treated as an external potential for the electrons of the system. When the Born-Oppenheimer approximation is facilitated, the electronic structure problem simplifies to the solution of Eq. 1.2 with the substitution of Eq. 1.8 for the Hamiltonian function. The nuclear positions \mathbf{R}_k are taken as variational parameters in the geometry optimization type calculations in which the calculated eigenvalue result is minimized by varying the parameters \mathbf{R}_k .

Analytical solutions of Eq. 1.2 is not possible for many electron quantum systems and thus numerical techniques are commonly used to find the solution. A natural attempt for numerically solving such an eigenvalue equation would be trying to diagonalize the Hamiltonian operator after calculating the matrix elements using some basis functions. However, since

the wavefunction is most of the time not separable into individual particle wavefunctions, the Hamiltonian operator of the composite system is a higher dimensional object for which an exact diagonalization procedure is not available. In the Hartree-Fock [6, 9] type approximate methods, the wavefunction is assumed to be separable and Eq. 1.2 is decomposed into single particle equations to simplify the problem.

An alternative technique for the solution of the electronic structure problem is calculating the time evolution of an arbitrary initial wavefunction according to the time dependent Schrödinger equation given in Eq. 1.1. Since the long time evolution process would yield the ground state solution of the quantum system, the ground state eigenvalue and eigenstate can be calculated using such an evolution. This technique can also be used for finding the solution for the ground state of the fermion systems or for any other excited states if the symmetry of the wavefunction for the desired state can be imposed on the time evolution process. The time dependent Schrödinger equation is transformed into an integral equation for finding the time evolution. However, calculations of the encountered integrals are very time consuming with grid techniques since the dimensionality of the integrals are very high [20]. Statistical sampling techniques reduce the computation times of such higher dimensional integrals many orders of magnitude. The diffusion Monte Carlo method [7, 8, 21], which is the main subject of this thesis work, is a genius statistical technique for finding the ground state eigenvalue using an evolution in imaginary time. Quantum Monte Carlo methods, using statistical sampling techniques for the solution of the electronic structure problem, will be discussed in the next section with a special emphasis on the diffusion Monte Carlo method.

1.2 Quantum Monte Carlo

Investigations of the electronic structure properties of quantum many-body systems require calculations along the multi-dimensional configuration spaces because of the inseparable wavefunctions inherent to the quantum mechanical systems as discussed in the previous section. Statistical sampling techniques are very useful for such investigations since a direct calculation using the grid techniques requires exponential increase in the computation time with increasing number of particles due to the multi-dimensional nature of the problem. An historical account of the usage of the statistical techniques for this purpose is given in the article of Metropolis [22] who is among the developers of the idea in the World War II years.

QMC [7, 8, 23, 24, 20, 25, 26] is a generic name for a variety of methods relying on the statistical sampling of the wavefunction to overcome the exponential scaling problem in the electronic structure calculations. Reviews of major QMC related articles in the literature are given in the 2007 year book of Anderson[27]. Variational Monte Carlo (VMC) [7, 8, 28, 29], Diffusion Monte Carlo (DMC) [7, 8, 21, 30], Green's function Monte Carlo (GFMC) [7, 31] and Path integral Monte Carlo (PIMC) [26, 32] are major QMC methods used for electronic structure calculations. The common methods, VMC and DMC will be reviewed in the subsequent sections after introductory information about the sampling techniques is given. The DMC method will be discussed more broadly since the developments in this thesis work are about this projector method.

1.2.1 Statistical sampling and the Metropolis algorithm

Selecting some representative points from a large population and generalizing the sample calculations for the all population is called sampling. Random walk [33, 34] is a widely used sampling technique and it is the basis for all QMC methods. This statistical technique is very useful for calculations involving multi-dimensional functions for which direct calculation is usually very exhaustive in terms of the computation effort. The Metropolis algorithm [7, 8, 33, 34, 35] is used for efficient samplings of arbitrary complex distribution functions. The advantage of the Metropolis algorithm is that the normalization of the distribution $D(\mathbf{x})$ is not have to be known for the sampling process. It generates sample points by using a random walk process according to a simple distribution $T(\mathbf{x})$ such as uniform or Gaussian distributions. The random walk steps are accepted or rejected according to a probability function calculated using the two points, before and after the random walk step:

$$P(\mathbf{x} \rightarrow \mathbf{x}') = \frac{T(\mathbf{x} \leftarrow \mathbf{x}')D(\mathbf{x}')}{T(\mathbf{x} \rightarrow \mathbf{x}')D(\mathbf{x})}, \quad (1.9)$$

where $T(\mathbf{x} \rightarrow \mathbf{x}')$ is the transition probability from the point \mathbf{x} to another point \mathbf{x}' in the configuration space. The acceptance probability is taken as unity if the numerical value of the above expression for the probability exceeds 1.0. When a symmetric function, such as a uniform or a gaussian function, is used for the distribution $T(\mathbf{x})$, the transition probabilities $T(\mathbf{x} \rightarrow \mathbf{x}')$ and $T(\mathbf{x} \leftarrow \mathbf{x}')$ become equal to each other and the probability expression simplifies to the fraction $D(\mathbf{x}')/D(\mathbf{x})$. Some number of initial walk steps depending on the step size should

be ignored if the initial point is chosen randomly because of the possibility that the initial points may be generated in a very low probability region of the configuration space. After these thermalization steps the generated points are expected to be distributed according to the distribution $D(\mathbf{x})$.

1.2.2 Monte Carlo integration

Evaluation of the multi-dimensional integrals is a common application of the statistical sampling technique described in the previous subsection. The Monte Carlo integration method [33, 34] relies on the separation of the integrand in two parts:

$$I = \int_{\Omega} D(\mathbf{x})R(\mathbf{x})d\mathbf{x} , \quad (1.10)$$

$D(\mathbf{x})$ being a normalized distribution function defined in the integration interval Ω and $R(\mathbf{x})$ is the remaining part of the integrand. $D(\mathbf{x})$ is sampled using the Metropolis algorithm and the numerical value of the integral is found with a certain statistical error by calculating and summing the values of $R(\mathbf{x})$ at N points generated according to the distribution $D(\mathbf{x})$, with an overall division factor of N :

$$I = \frac{1}{N} \sum_{i=1}^N R(\mathbf{x}_i) . \quad (1.11)$$

The statistical error in the calculated result is inversely proportional to \sqrt{N} . Therefore the result can be found with desired precision by increasing the number of sample points N . The Monte Carlo integration technique is advantageous compared to deterministic grid techniques for configuration spaces having dimensionality four or larger [34].

1.2.3 Variational Monte Carlo

VMC [7, 8, 28, 29] is a direct application of the Monte Carlo integration technique. It facilitates the variational principle (Section 1.1.2) which states that the energy expectation value computed from an arbitrary trial wavefunction $\Psi_T(\mathbf{x})$ is always greater than or equal to the ground state eigenvalue E_0 :

$$\langle E \rangle = \frac{\langle \Psi_T(\mathbf{x}) | \hat{H}_e | \Psi_T(\mathbf{x}) \rangle}{\langle \Psi_T(\mathbf{x}) | \Psi_T(\mathbf{x}) \rangle} \geq E_0 . \quad (1.12)$$

In the VMC method, the parameters of the trial wavefunction are optimized for finding the ground state eigenstate and eigenvalue of the quantum system by a minimization of the energy expectation value calculated using the Monte Carlo integration. The integrand is separated in two parts as follows:

$$\langle E \rangle = \frac{\int \Psi_T^*(\mathbf{x}) \hat{H}_e \Psi_T(\mathbf{x}) d\mathbf{x}}{\int \Psi_T^*(\mathbf{x}) \Psi_T(\mathbf{x}) d\mathbf{x}} = \frac{\int |\Psi_T(\mathbf{x})|^2 [\Psi_T(\mathbf{x})^{-1} \hat{H}_e \Psi_T(\mathbf{x})] d\mathbf{x}}{\int |\Psi_T(\mathbf{x})|^2 d\mathbf{x}} , \quad (1.13)$$

where $|\Psi_T(\mathbf{x})|^2 / \int |\Psi_T(\mathbf{x})|^2 d\mathbf{x}$ is chosen as the positive definite probability distribution $D(\mathbf{x})$, according to which the sample points are generated. The remaining part of the integrand is identified as $R(\mathbf{x})$ and the integration is carried out according to the formula described in Eq. 1.11.

In order to increase the efficiency of the method the optimization can be carried out by the minimization of the variance of the local energy:

$$E_L(\mathbf{x}) = \Psi_T(\mathbf{x})^{-1} \hat{H}_e \Psi_T(\mathbf{x}) , \quad (1.14)$$

for which the variational principle also holds. The global minimum value of the E_L variance is a known value (zero) as opposed to the global minimum of the energy expectation value, making the variance optimization more advantageous. In addition, the variance optimization is usually done with less number of iterations compared to the energy expectation value optimization.

If the minimization of the energy or E_L variance is carried out using a local optimization routine such as the Newton's method or conjugate gradients [36], the optimized parameter set would most probably represent a local minimum, reducing the quality of the obtained trial wavefunction. Therefore, global optimization procedures such as simulated annealing [37] or genetic algorithms [38] should be facilitated in the VMC optimization of the trial wavefunction.

VMC is most of the time used for wavefunction optimization before a DMC calculation [30].

However, it is also used standalone to calculate the ground state properties of various quantum systems [29] . When the fermions are studied with VMC, the antisymmetry condition should be imposed on the trial wavefunction and this condition should be preserved during the parameter optimization procedure. Slater determinants [39] are usually preferred for the imposition of the fermion antisymmetry in the trial wavefunctions which are discussed in Section 1.4.

1.2.4 Diffusion process as random walk

The diffusion equation:

$$\partial_t f(\mathbf{x}, t) = \kappa \nabla^2 f(\mathbf{x}, t) , \quad (1.15)$$

describes the time evolution of the density function $f(\mathbf{x}, t)$, κ being a real constant. The meaning of Eq. 1.15 can be clarified using a model problem in which an ensemble of hard spheres moving on straight lines with constant velocities in empty space. Masses, radii and speeds of the all spheres are taken as equal to each other for convenience. Each hard sphere has a certain position \mathbf{x}_i and velocity vector \mathbf{v}_i at $t = 0$ instance. These hard spheres may encounter during their motion and their velocity vectors change direction in these particle collisions according to the momentum conservation rule. It would be very time consuming to calculate the positions and velocities of the spheres at some later time t_f because of the collisions. However, if we are just concerned with the density function of the spheres at a specific instance we can use Eq. 1.15 since the above described motion of spheres is a diffusion process.

Finding the exact solution of Eq. 1.15 for an arbitrary initial density function $f(\mathbf{x}, 0)$ is mostly very challenging. However, Eq. 1.15 can be solved in a simpler way with certain statistical error using the stochastic process of random walk in which the spheres move randomly according to a Gaussian distribution function without colliding each other. This random motion is usually implemented by random walk steps whose direction are arbitrary and step sizes are chosen randomly according to a Gaussian distribution function. The connection between the Gaussian random walk and the diffusion equation is better observed if Eq. 1.15 is converted to an integral equation [34]. The DMC method discussed in Section 1.2.5 is based on this

stochastic solution of the diffusion equation.

1.2.5 Diffusion Monte Carlo

The projector QMC methods [8, 23, 34, 40] find the ground state of the Schrödinger equation by time evolving a starting wavefunction. The most common projector method DMC [7, 8, 21, 30] applies an evolution in imaginary time using a propagator valid for short times. The DMC method relies on the fact that the form of the Schrödinger equation in imaginary time (Wick rotation of time: $\tau = it$) being a diffusion equation with a source term:

$$\partial_\tau \Psi(\mathbf{x}, \tau) = \frac{1}{2} \nabla^2 \Psi(\mathbf{x}, \tau) - [V(\mathbf{x}) - E_R] \Psi(\mathbf{x}, \tau), \quad (1.16)$$

where E_R , the *reference energy*, is an energy shift whose effect will be clarified below. Solution of the above equation can be written in terms of the eigenfunctions Φ_n as,

$$\Psi(\mathbf{x}, \tau) = \sum_{n=0}^{\infty} c_n \Phi_n e^{-(E_n - E_R)\tau}, \quad (1.17)$$

where E_n 's are the corresponding eigenvalues and c_n denote the overlap parameters:

$$c_n = \langle \Phi_n | \Psi(\mathbf{x}, \tau) \rangle. \quad (1.18)$$

In the long τ limit, the exponential factor causes the excited state components to die out faster than the ground state component whose eigenvalue E_0 is lower than the excited state eigenvalues. Consequently, the wavefunction becomes dominated by the ground state component when the wavefunction is evolved sufficiently long in the imaginary time.

For short imaginary time intervals $\Delta\tau$, the evolution of the wavefunction can be calculated as,

$$\Psi(\mathbf{x}, \tau_0 + \Delta\tau) = \int d\mathbf{x} P(\mathbf{x}, \mathbf{x}_0) W(\mathbf{x}) \Psi(\mathbf{x}_0, \tau_0), \quad (1.19)$$

where the kinetic energy related term P is the diffusion kernel:

$$P(\mathbf{x}, \mathbf{x}_0) = \left(\frac{1}{2\pi\Delta\tau} \right)^{3N/2} \exp\left(- \frac{(\mathbf{x} - \mathbf{x}_0)^2}{2\Delta\tau} \right), \quad (1.20)$$

and the source related W term is defined as,

$$W(\mathbf{x}) = \exp\left(- [V(\mathbf{x}) - E_R]\Delta\tau \right). \quad (1.21)$$

In the DMC method, the short time propagation of the wavefunction is iterated for a sufficiently long time in order to find the ground state of the system. A starting wavefunction is sampled with a certain number of points (also called as *walkers*) in the configuration space. In each iteration, all walkers are subjected to a Gaussian random walk step due to the diffusion kernel P as,

$$x'_i = x_i + \rho_i, \quad (1.22)$$

where x_i 's are the walker components in the configuration space and ρ_i 's are random numbers chosen from a Gaussian distribution with mean zero and variance $\sqrt{\Delta\tau}$. The walkers are also subjected to a branching process due to the W term which can be approximated in the small $\Delta\tau$ limit as

$$W(\mathbf{x}) = 1 - [V(\mathbf{x}) - E_R]\Delta\tau. \quad (1.23)$$

Walker weights are multiplied by $(W(\mathbf{x}) + u)$, u being a uniform random number between zero and unity. Alternatively, the walkers may be replicated by n walkers using the same criterion as,

$$n = \text{int}(W(\mathbf{x}) + u). \quad (1.24)$$

Replication process enables a more stable algorithm compared to the weight multiplication which results in huge differences between walker weights. These two alternatives may be used together in which walker weights are modified in a certain range and the walkers replicate or die when their weights get out of this chosen range. An upper limit on the factor $(W(\mathbf{x}) + u)$ or

on the replication number n would avoid instabilities especially in the beginning of the DMC run. An illustration of the imaginary time evolution including the diffusion and the branching processes are given in Figure 1.1 [8].

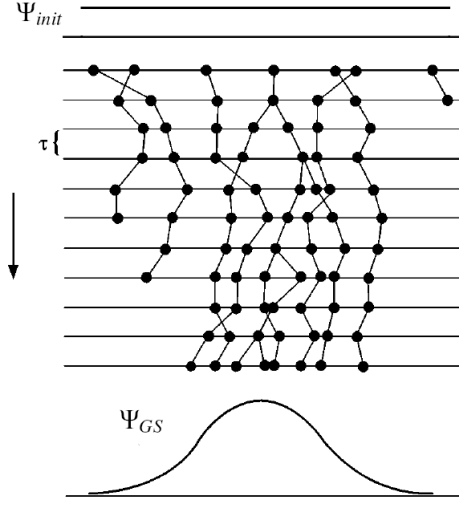


Figure 1.1: Illustration of the imaginary time evolution in DMC method. Adapted from [8].

Total number of walkers, which determines the normalization of the wavefunction, is altered as a result of the branching process. The reference energy E_R which is applied as an energy shift in the imaginary time Schrödinger equation (Eq. 1.16) is used to satisfy the normalization condition of the wavefunction. Numerical value of E_R is modified as,

$$E_R = \langle V \rangle + \frac{\alpha}{\Delta\tau} \left(1 - \frac{N}{N_0} \right), \quad (1.25)$$

in order to adjust the rate of the branching process in a way to keep the total number of walkers constant. N and N_0 are the current and desired number of walkers respectively and α is a parameter determining the strength of the adjustments. The walker potential energy average $\langle V \rangle$ corresponds to the energy expectation value calculated from the walker distribution $\Psi(\mathbf{x}, \tau)$. This correspondence is seen by the integration of the eigenvalue equation (Eq. 1.2) over the whole configuration space:

$$\begin{aligned} E \int \Psi(\mathbf{x}, \tau) d\mathbf{x} &= \int \hat{H}_e \Psi(\mathbf{x}, \tau) d\mathbf{x} \\ &= -\frac{1}{2} \int_{\partial\Omega} \nabla \Psi(\mathbf{x}, \tau) \cdot d\mathbf{S} + \int V(\mathbf{x}) \Psi(\mathbf{x}, \tau) d\mathbf{x}, \end{aligned} \quad (1.26)$$

where divergence theorem is used in the first term of the second line. This term is about the walker flow at the boundaries and it vanishes since the solution is carried out in the whole configuration space. Therefore, the energy expectation value becomes:

$$E = \frac{\int V(\mathbf{x})\Psi(\mathbf{x}, \tau)d\mathbf{x}}{\int \Psi(\mathbf{x}, \tau)d\mathbf{x}} = \langle V \rangle . \quad (1.27)$$

The energy expectation value calculation described above is valid only when the walker distribution represents an eigenvalue of the system and thus the variational principle is not valid. However, absence of the variational principle does not pose a problem for the described pure DMC procedure since the walker distribution is shown to evolve through the ground state eigenstate in Eq. 1.17. A time average of the walker potential energy averages should be taken after a sufficiently long thermalization period in order to compute the ground state eigenvalue of the system.

In the DMC method the wavefunction of the quantum system is assumed to be a real valued function even though it is in general complex valued. This assumption is valid for systems investigated in the condensed matter area having time reversal symmetry [8] since the wavefunction for such systems can be written as a real valued function. Generalization of the DMC method for treating complex wavefunctions is also possible [41].

The time evolution of the wavefunction in the DMC method is for the spatial part of the wavefunction only. The effect of the spin variables should be included by some other means. The fermion sign problem which will be discussed in Section 1.2.7 is about the treatment of the spin variables for fermions.

1.2.6 Importance sampling DMC

Efficiency of the DMC method can be improved by the application of the importance sampling transformation [7, 8, 42] on Eq. 1.1 via multiplication by a trial wavefunction $\Psi_T(\mathbf{x})$:

$$\Psi_T(\mathbf{x}) \partial_\tau \Psi(\mathbf{x}, \tau) = \frac{1}{2} \Psi_T(\mathbf{x}) \nabla^2 \Psi(\mathbf{x}, \tau) - [V(\mathbf{x}) - E_R] \Psi(\mathbf{x}, \tau) \Psi_T(\mathbf{x}) . \quad (1.28)$$

Above equation can be organized as follows using the definition $f(\mathbf{x}, \tau) = \Psi(\mathbf{x}, \tau) \Psi_T(\mathbf{x})$

together with the definitions of the local energy (Eq. 1.14) and the *drift velocity* $\mathbf{v}_D(\mathbf{x}) = \Psi_T(\mathbf{x})^{-1} \nabla \Psi_T(\mathbf{x})$:

$$\partial_\tau f(\mathbf{x}, \tau) = \frac{1}{2} \nabla^2 f(\mathbf{x}, \tau) - \nabla \cdot [\mathbf{v}_D(\mathbf{x}) f(\mathbf{x}, \tau)] - [E_L(\mathbf{x}) - E_R] f(\mathbf{x}, \tau). \quad (1.29)$$

The diffusion kernel (Eq. 1.20) and the branching kernel (Eq. 1.21) should be modified as the following for the importance sampling DMC simulation:

$$P(\mathbf{x}, \mathbf{x}_0) = \left(\frac{1}{2\pi\Delta\tau} \right)^{3N/2} \exp\left(- \frac{[\mathbf{x} - \mathbf{x}_0 - \Delta\tau \mathbf{v}_D(\mathbf{x}_0)]^2}{2\Delta\tau} \right), \quad (1.30)$$

$$W(\mathbf{x}) = \exp\left(- [E_L(\mathbf{x}) - E_R]\Delta\tau \right). \quad (1.31)$$

For the $P(\mathbf{x}, \mathbf{x}_0)$ part, a Gaussian random walk as described in Eq. 1.22 is applied together with a drift motion according to the vector $\Delta\tau \mathbf{v}_D(\mathbf{x}_0)$. The DMC branching process described in Section 1.2.5 due to the $W(\mathbf{x})$ term is carried out wrt the local energy E_L instead of the potential energy function V .

The energy expectation value for the importance sampling DMC is calculated using the fact that the walker distribution in this case converges to the mixed state $\Psi_{GS}(\mathbf{x}) \Psi_T(\mathbf{x})$, $\Psi_{GS}(\mathbf{x})$ being the ground state of the studied system. The ground state energy is calculated using the mixed estimator [8]:

$$\langle E \rangle = \frac{\langle \Psi_0(\mathbf{x}) | \hat{H}_e | \Psi_T(\mathbf{x}) \rangle}{\langle \Psi_0(\mathbf{x}) | \Psi_T(\mathbf{x}) \rangle}, \quad (1.32)$$

which can be written in terms of the function $f(\mathbf{x}, \tau)$ and the local energy $E_L(\mathbf{x})$ as:

$$\langle E \rangle = \lim_{\tau \rightarrow \infty} \frac{\int f(\mathbf{x}, \tau) E_L(\mathbf{x}) d\mathbf{x}}{\int f(\mathbf{x}, \tau) d\mathbf{x}}. \quad (1.33)$$

This expression for the energy is in a form suitable for Monte Carlo integration described in Section 1.2.2 and it can be calculated using the walker distribution $f(\mathbf{x}, \tau)$ as:

$$\langle E \rangle = \frac{1}{N} \sum_n E_L(\mathbf{x}_n), \quad (1.34)$$

where the sum is over the all walkers of total number N . The above sum should be time averaged after a thermalization period which is necessary for the walker distribution's convergence to the mixed state $\Psi_{GS}(\mathbf{x}) \Psi_T(\mathbf{x})$.

The importance sampling transformation replaces the potential energy function V with the local energy E_L in the branching and the energy calculations of DMC. Usage of the local energy in these processes is very advantageous compared to the potential energy function which has large fluctuations and divergences. The fluctuation amount in E_L depends on the quality of the trial wavefunction $\Psi_T(\mathbf{x})$ and it is several orders of magnitude less than the fluctuation amount of the potential energy function when the trial wavefunction is not extremely bad. Therefore the importance sampling transformation reduces the statistical error of the DMC method several times and enables faster computations of large systems. Fermion trial wavefunctions used in the QMC computations are discussed in Section 1.4.

1.2.7 Fermion sign problem (FSP) in DMC

The DMC method described in the previous section, in its pure form, cannot be used for fermions since the lowest lying eigenstate of the Schrödinger equation is always symmetric under identical particle permutations, describing boson statistics. The walker distribution tends to the symmetric bosonic ground state having the lowest energy eigenvalue in the imaginary time evolution because of the exponential term in the Eq. 1.17:

$$\Psi(\mathbf{x}, \tau) = \sum_{n=0}^{\infty} c_n \Phi_n e^{-(E_n - E_R)\tau}. \quad (1.35)$$

Consequently, a symmetric noise in the walker distribution arises and increases exponentially fast even if the initial walker distribution does not have a symmetric component [40, 43]. The DMC reference energy may be used to ensure the existence of a certain antisymmetric component, causing an exponential increase in the total number of walkers which is not feasible in terms of the computational effort. The exponential decrease of the signal to noise ratio problem is still not resolved and the method is unstable.

However, as stated in Section 1.1.4, the wavefunction is composed of spin and spatial parts and the problem for fermions does not occur if the spin part of the wavefunction is fully antisymmetric in which case the spatial part is symmetric, allowing a straight forward DMC calculation. Unfortunately the ground states of the molecular systems have antisymmetric spatial parts except a few simple cases such as the helium atom.

Some methods have been suggested for fermion systems having FSP in the last couple of decades to overcome the exponential noise increase problem. However, no exact solution of FSP could be developed and also NP Hardness of the problem was suggested [44]. An approximate technique, called as the fixed-node approximation [10], is widely used for the QMC applications involving more than a few fermions because of the absence of an exact solution of FSP. This approximate technique and suggested exact methods will be discussed in the next subsection.

1.2.8 Fixed-node approximation

Ground state of the Schrödinger equation for any fermion system has a nodal surface separating positive and negative valued wavefunction regions as opposed to the bosonic ground state which does not alternate sign. This nodal surface is a $d \times n - 1$ dimensional hypersurface [45, 46] in the $d \times n$ dimensional configuration space where d and n denote the number of spatial dimensions and the number of identical particles respectively. In the fixed-node DMC [7, 8, 10], the nodal surface of the fermionic ground state wavefunction is determined by a preliminary calculation and used as the boundary condition in the DMC computation. The computation is carried out in a constant sign wavefunction region and the outgoing walkers are killed or avoided in order to have a zero valued wavefunction on the nodal surface. The fixed-node technique is in principle exact when the true nodal surface is known. However, there is no general procedure for the determination of the $d \times n - 1$ dimensional nodal hypersurface and thus an approximate nodal surface is used for which the calculated DMC result has certain systematic error.

When the fixed-node technique is used in the pure DMC without using the importance sampling transformation, the walkers that pass out of the nodal region should be killed in order to keep the walkers inside. This procedure causes a small bias in the population control mechanism using the reference energy and also in the calculated expectation value result. In the

importance sampling DMC this problem is avoided automatically to a great extent. In this case, the drift velocity directs the walkers to the regions where the trial wavefunction has large values and it pushes the walkers away from the nodal surface where the trial wavefunction vanishes. Therefore, the walkers are ideally trapped in the nodal region automatically. However, a small amount of walkers may still go out because of the discretized time steps used in the DMC calculations. Killing these outgoing walkers causes a small bias also for this case and a better procedure to overcome this problem is to reject the walker moves that pass through the nodal surface.

In the work of Manten and Luchow [47], the accuracy of the fixed-node DMC with Hartree-Fock trial wavefunctions is compared with coupled cluster calculations. The accuracies of the two methods are found to be approximately same in this comparison. The fixed-node approximation is currently a standard tool used in the QMC calculations of relatively larger systems [30, 48, 49, 50, 51, 52]. Publicly available QMC codes such as CASINO [53] and ZORI [54] facilitate this technique for making calculations on large molecular systems.

1.3 DMC Beyond the Fixed-node Approximation

The fixed-node DMC, described in the previous section, is a highly accurate tool for electronic structure calculations and it is widely used in nano scale applications demanding high accuracy. However, the fixed-node technique is not exact because of the approximate nodal surface of the trial wavefunction used for imposing the antisymmetry constraint. Solutions of the node problem in the DMC method without using the fixed-node approximation are being searched for many decades. Techniques and strategies beyond the fixed-node approximation will be discussed below as separate titles.

1.3.1 Released-node technique

The released-node technique [55] is the first step towards an exact DMC method in which the walkers are allowed to pass through the nodal surface and they get plus and minus signs as a natural consequence of the sign alternating wavefunction [56]. Walker signs change according to the sign of the trial wavefunction and minus signed walkers give negative weights in the energy calculation. The wavefunction Ψ in the released-node technique is represented by the

difference of two positive functions as:

$$\Psi = \Psi^+ - \Psi^- , \quad (1.36)$$

where Ψ^+ and Ψ^- are sampled by plus and minus signed walkers respectively.

This basic extension of the fixed-node approximation is not stable since the walker distribution prefers the bosonic ground state instead of the desired antisymmetric function. The DMC reference energy E_R may be used to stabilize the difference of the number of plus and minus signed walkers in order to avoid the diminishing of the antisymmetric contribution. However, the plus and minus signed walker populations constantly increase in this case and these two walker populations separately go to the bosonic ground state in the long τ limit. Alternatively, the total population may be kept constant in which case the antisymmetric component vanishes completely in the long run.

The fermionic ground state energy can still be extracted if a high quality trial wavefunction is available. The plus and minus signed walker distributions are initialized in two different nodal regions according to the trial wavefunction and the released-node technique is applied with this initial configuration. The expectation value is calculated from the antisymmetric component before it becomes insignificant beside the noise of the symmetric ground state component. This technique, also called as *transient estimate*, is widely used to improve the accuracy following a fixed-node DMC calculation. Some works that used the transient estimate method to calculate various properties of small systems are given in the references [57, 58, 59, 60, 61, 62]. However, applicability of this method is limited because of the instability inherit in its methodology.

1.3.2 Plus minus cancellation methods

A strategy to avoid the instability problem encountered in the released-node technique is developed by Arnow et al. [56] in which opposite signed walkers cancel each other when they encounter in the random walk process [63, 64, 65]. The cancellation process does not cause a biased expectation value result since the average future contribution of the two opposite signed walkers vanishes after they share the same position. In practice, two walkers never share the same position exactly and thus walkers in a close proximity cancel each other bring-

ing some bias to the energy expectation value. In this way the cancellation process can be used to stabilize the numbers of plus and minus signed walkers when the reference energy is used to preserve a constant difference between the two population sizes. This strategy allows stable and almost exact DMC calculations for small fermion systems. However, the cancellation strategy does not work for systems including more than a few identical fermions because of the increase in the dimensionality of the configuration space for which the walker encounter rate is very low due to the sparsity of the walkers. The proximity threshold should be increased very much for such higher dimensional configuration spaces to have an effective cancellation process, bringing huge systematic error to the expectation value result. In order to avoid the systematic error, the number of walkers should increase exponentially as the number of configuration space dimension (number of identical particles) increases linearly. This exponential scaling increase of the number of walkers and the computational effort may be originating from the suggested NP Hard nature of the fermion sign problem [44].

1.3.3 Correlated walk of opposite signed walkers

The cancellations of opposite signed walkers described in the previous subsection can be carried out in a more exact and efficient way by correlating the diffusion process of plus and minus signed walkers [66, 67]. The diffusion process in this technique is carried out using pairs of walkers composed of one plus and one minus signed walker and the Gaussian walk vector of one member of the pair is obtained by reflecting the other member's vector in the perpendicular bisector of $\mathbf{x}_1 - \mathbf{x}_2$, the vector connecting the two walkers. In this way, the random walk process for the paired walkers becomes equivalent to a 1D random walk and their encounter probability increases several times depending on the dimensionality of the configuration space [43].

Another advantage of the correlated walk process is that it allows exact cancellation of opposite signed walkers without need for a proximity threshold. The Gaussian random walk vectors of the pair walkers coincide easily in the correlated walk case and this coincidence is taken as the condition for the cancellation. There still comes a small bias because of the discrete time steps but it can be made arbitrarily small by lowering the DMC time step value.

1.3.4 Non-symmetric guiding functions and the fermion Monte Carlo

An enhancement on the correlated walk process described in the previous subsection was developed by Kalos and Pederiva [67], using non-symmetric guiding functions in the importance sampling DMC. In this technique which is called as the fermion Monte Carlo (FMC), two guiding function are used for the plus and the minus signed walkers separately for the importance sampling process. These guiding functions are composed of one symmetric and one antisymmetric function which are defined as:

$$\Psi_G^\pm(\mathbf{x}) = \sqrt{\Psi_S^2(\mathbf{x}) + c^2\Psi_A^2(\mathbf{x})} \pm c\Psi_A(\mathbf{x}) , \quad (1.37)$$

where $\Psi_S(\mathbf{x})$ and $\Psi_A(\mathbf{x})$ are the symmetric and the antisymmetric functions respectively and c is the mixing coefficient. When the importance sampling is applied with such different guiding functions for the two walker populations, the cancellation rate and the stability of the non fixed-node DMC can be increased. However, it was proven that the FMC algorithm has certain population control bias due to the usage of the non symmetric guiding functions and therefore it loses the exactness for increasing the stability [43]. Therefore, the fermion sign problem is still unresolved and application of the exact cancellation methods to the relatively large systems is not possible.

1.3.5 Using permutation symmerty

Quantum mechanical wavefunction of the identical particles repeats a pattern exactly or with a sign inversion as discussed in Section 1.1.3. This property of the permutation symmetry can be used to shrink the configuration space volume several times, increasing the encounter rate of the opposite signed walkers. In this technique, the DMC computation is carried out in a single *permutation cell* which is the repeating unit cell of the quantum mechanical wavefunction [63, 68]. The outgoing walkers are taken back to inside by the application of the necessary particle permutations. This boundary condition as permuting back the outgoing walkers represents a situation where the wavefunction values at the two sides of the boundary are the same and therefore it is suitable for the symmetric boson wavefunctions. For the fermion case, a sign inversion of the wavefunction occurs when the permutation cell boundary is passed over and the appropriate action for the outgoing walker is permuting back as for the

boson case and reversing the sign of the walker if an odd number of particle permutations are needed to take the walker back inside the permutation cell.

The permutation cell choice is not unique for a given quantum system but it can be defined in many ways. A simple definition applicable to all systems is sorting a certain space dimension of the all identical particles [68]. A walker gets out of the permutation cell when the chosen space dimensions of the particles become unsorted and it can be taken inside by re-sorting the particles using appropriate particle permutations.

The above definition of the permutation cell with the sort operation on a space dimension of the particles results in a constant sign permutation cell only for fermions interacting with harmonic oscillator type potential function. However, in general, when this permutation cell definition is used for the fermions, the wavefunction would change sign in a permutation cell region. If a constant sign permutation region (like a nodal region) is desired, the nodal regions of the DFT wavefunctions can be used since they have the permutation cell property as stated in the Ceperley's work on the wavefunction nodes [69].

1.3.6 Other Strategies towards the solution of FSP

Beside the strategies previously discussed, there are many articles in the literature suggesting solutions to the fermion sign problem in the DMC method. These solution attempts mostly combine some of the previously described strategies with some other tricks. Some of these attempts are discussed here briefly.

Anderson et al. [63] developed a cancellation facilitating algorithm which uses the permutation symmetry to bound the simulation region. The cancellation regime of Arnow et al. [56] is improved in this work: The accuracy of the cancellation regime is increased using overlaps of the walker distribution functions and the cancellation rate is enhanced by some tricks such as *self cancellations* and *multiple cancellations*. This work of Anderson et al. uses GFMC method. However, their developments about the sign problem are applicable also to the DMC method.

In the work of Bianchi et al. [70] the walkers are represented by Gaussian functions instead of usual Dirac delta functions in order to improve the cancellation process of opposite signed walkers. The Gaussian representation reduces the problem arising from the sparse walker

distribution to some extent.

Mishchenko added a potential term to the Hamiltonian function to alter the eigenvalues of the symmetric solutions of the Schrödinger equation [71]. The lowest lying state becomes antisymmetric with the addition of the non local potential term $A(1+\pi)$ where $\pi \Psi(\mathbf{x}) = \Psi(-\mathbf{x})$ and A is a constant. However, the method still needs the cancellations of opposite signed walkers and it includes a complicated process for dynamically determining the nodal surface.

Thom and Alavi developed a method in which the walkers reside in the discretized Slater determinant space instead of the position space continuum [72]. The cancellations of opposite signed walkers can be carried out more efficiently in a such discretized configuration space. However, the sign problem is still not resolved for large systems and the exponential increase in the number of walkers is still necessary for the exact solution.

In the auxiliary-field methods [73, 74], the interaction between the electrons are replaced by an interaction between the electrons and a random potential. Therefore, the many-body problem is reduced to a mean field problem which is easier to solve.

The recent method of Reboredo et al. [75] is based on the trial wavefunction optimization during the fixed-node DMC calculation. In this scheme, the nodal surface and the calculated result is improved iteratively.

These techniques and strategies discussed above increase the stability of the non fixed-node DMC to some extent. However, none of them resolve the problem without introducing a systematic bias in the computed result. Therefore, the DMC method is not applicable to large fermion systems without using the fixed-node approximation.

1.4 Fermion Trial Wavefunctions

Quality of the trial wavefunction is an important factor affecting the accuracy and the precision of the expectation value results obtained by the QMC calculations. The form and the parameters of the trial wavefunction directly determine the quality of a VMC calculation result. The pure DMC calculation result in principle does not rely on the trial wavefunction. However, trial wavefunctions are used in importance sampling DMC to reduce the statistical error of the calculation and their importance increase as the studied system becomes larger.

The nodal hypersurface of the trial wavefunction is used in the fixed-node DMC for the imposition of the antisymmetry condition and the quality of the trial wavefunction nodal surface is essential for the accuracy of the obtained result. Most of the current fermionic QMC applications use importance sampling DMC with fixed-node approximation for which the quality of the trial wavefunction and its nodal hyper surface determines the accuracy and the precision of the calculated expectation value results.

The QMC methods of the all kinds require evaluation of the trial wavefunction value many times during the computation. Therefore, a complicated trial wavefunction form would slow down the computation significantly. Considering the tradeoff between the speed and the accuracy, the trial wavefunctions used in the QMC applications are usually composed of a single Slater determinant and a symmetric Jastrow factor:

$$\Psi_T(\mathbf{x}) = e^{J(\mathbf{x})} \times D(\mathbf{x}) . \quad (1.38)$$

The Slater determinant $D(\mathbf{x})$ is formed by one electron orbitals obtained from a Hartree-Fock or DFT calculation. The Jastrow factor $J(\mathbf{x})$ is responsible for the electron-electron and electron-nucleus correlation effects and the cusp conditions. The parameters which are optimized during the VMC computation reside in the Jastrow factor if a single Slater determinant is used in the trial wavefunction and these parameters do not affect the nodal hypersurface which is determined by the Slater determinant $D(\mathbf{x})$. If an improvement of the nodal hypersurface is intended in the VMC optimization, a linear combination of Slater determinants is used having coefficient parameters for each determinant.

The spin variables can be excluded from the trial wavefunction if a spin independent operator is used in the expectation value calculation [76]. In such a case, the function $D(\mathbf{x})$ can be decomposed into two determinants, one for the up spin electrons and the other for the down spin electrons:

$$D(\mathbf{x}) = D_u(\mathbf{x}') D_d(\mathbf{x}') , \quad (1.39)$$

where the sub-indices u and d denote the up spin electrons and the down spin electrons respectively and the vector \mathbf{x}' does not include the spin variables. Such a decomposition is

advantageous since evaluation of the large determinant $D(\mathbf{x})$ is harder than evaluations of two smaller determinants and also a summation over the spin variables is no longer necessary.

The trial wavefunctions used in this thesis work are formed by slightly disturbing the exact analytical solutions if they are available. When the exact solution is not known, a high quality approximate wavefunction is found from the literature. Therefore, no preliminary Hartree-Fock or DFT calculations are carried out before the QMC calculations carried out for testing the developments discussed in the next chapter.

CHAPTER 2

WAVEFUNCTION CORRECTION SCHEME FOR NON FIXED-NODE DMC

A technique, called as the wavefunction correction scheme, was developed around three decades ago to reduce the statistical error in the DMC calculations by Anderson and Freihaut [77]. This technique was used mostly in boson calculations and also once in a fixed-node fermion calculation. However, the correction scheme did not become widespread in the QMC community because of the problems about its large scale applicability. It reduces the stability of the DMC method for relatively larger systems by introducing minus signed walkers in to boson and fixed-node fermion calculations.

In this chapter of the thesis work, the application of the wavefunction correction technique to the non fixed-node DMC method is discussed. The purpose of such an application is to reduce the statistical error bars in such calculations. The correction scheme may find its application in this type of QMC calculations since the non fixed-node DMC calculations already have the large scale applicability problem as discussed in Section 1.2.7. A stable non fixed-node algorithm which becomes possible with some modifications on the correction scheme will also be discussed. The reasons of the accuracy reduction in the applications of this stable algorithm will be investigated with some benchmark calculations.

2.1 Wavefunction Correction Scheme

The DMC method is modified for making corrections on a given trial wavefunction in the wavefunction correction framework. The difference $[\Phi(\mathbf{x}, \tau)]$ between the true ground state wavefunction $\Psi(\mathbf{x}, \tau)$ and the trial wavefunction $\Psi_T(\mathbf{x})$ is sampled in the correction scheme

DMC calculations instead of the ground state wavefunction itself. This technique was used as an efficiency improvement mostly in the DMC calculations of bosons by its developers [77, 78, 79]. It was also used in the fixed-node DMC calculation of the water molecule which has fermionic nature [79].

For comprehending the modifications on the DMC methodology due to the wavefunction correction technique, it is necessary to substitute $\Phi(\mathbf{x}, \tau) + \Psi_T(\mathbf{x})$, the sum of the difference function and the trial wave function, for the wavefunction $\Psi(\mathbf{x}, \tau)$ in the imaginary time Schrödinger equation (Eq. 1.16):

$$\partial_\tau \Phi(\mathbf{x}, \tau) = \frac{1}{2} \nabla^2 [\Phi(\mathbf{x}, \tau) + \Psi_T(\mathbf{x})] - [V(\mathbf{x}) - E_R] [\Phi(\mathbf{x}, \tau) + \Psi_T(\mathbf{x})] , \quad (2.1)$$

which can be simplified using the local energy $E_L(\mathbf{x}) = \hat{H}_e \Psi_T(\mathbf{x}) / \Psi_T(\mathbf{x})$ as follows:

$$\partial_\tau \Phi(\mathbf{x}, \tau) = \frac{1}{2} \nabla^2 \Phi(\mathbf{x}, \tau) - [V(\mathbf{x}) - E_R] \Phi(\mathbf{x}, \tau) - [E_L(\mathbf{x}) - E_R] \Psi_T(\mathbf{x}) . \quad (2.2)$$

The wavefunction correction technique is illustrated in Figure 2.1. The difference function $\Psi_{GS}(\mathbf{x}) - \Psi_T(\mathbf{x})$ which is plotted in this figure is sampled in the correction scheme DMC calculations instead of the ground state wavefunction itself.

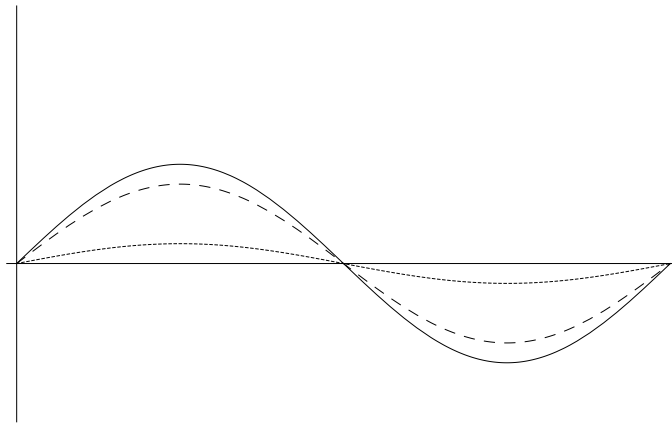


Figure 2.1: **Dashed Line:** Trial wavefunction $\Psi_T(\mathbf{x})$, **Solid Line:** Ground state wavefunction $\Psi_{GS}(\mathbf{x})$, **Dotted Line:** Difference function $\Psi_{GS}(\mathbf{x}) - \Psi_T(\mathbf{x})$.

2.1.1 Vacuum branchings

Eq. 2.2 is the same as Eq. 1.16 except the last term which is about the trial wavefunction being corrected. In the correction scheme calculations, this extra term is included in the DMC simulation as an extra source term and it is simulated by an extra branching process called in our works as the *vacuum branchings*. A plus or minus signed walker may be added to the walker population according to the position of the vacuum branching. These extra branchings are carried out at arbitrary positions in the configuration space with a uniform distribution in the original work of Anderson and Freihaut [77]. However, the vacuum branchings may be applied in a more efficient way using the Metropolis algorithm [80]: Some number of points are generated according to the function $\Psi_T(\mathbf{x})$ using the Metropolis algorithm and the branching factors are calculated with respect to the factor $[E_L(\mathbf{x}) - E_R]$ as follows:

$$W(\mathbf{x}) = 1 - [E_L(\mathbf{x}) - E_R]\Delta\tau . \quad (2.3)$$

The trial wavefunction $\Psi_T(\mathbf{x})$ should be non negative for such an application of the vacuum branchings and this condition is satisfied for the boson systems and also for the fixed-node fermion calculations. Application of the vacuum branchings in the non fixed-node calculations will be discussed in the next section. The reference energy E_R controls also the rate of the vacuum branchings beside the usual walker branchings.

2.1.2 Amplitude ratio parameter

The amplitude of the trial wavefunction is an important factor of the correction scheme calculations together with the stabilized value of the number of walkers which determines the wavefunction amplitude in the usual DMC [80]. The ratio of the trial wavefunction amplitude to the number of walkers from each sign (r_n) determines the efficiency improvement observed in the correction scheme calculations. When r_n increases, the efficiency also increases since the contribution of the walker population in the energy calculation and thus the variance of the computation decreases. This parameter of the method can be increased when the trial wavefunction gets closer to the true ground state wavefunction. However, r_n value should be determined with care since a full correction cannot be possible when its value becomes too high. The value of the parameter should be set to the highest value allowing the full correction

and this value can be guessed according to the quality of the trial wavefunction. Its value may be further optimized using the fact that a bias in the expectation value starts to occur beyond the optimum value. The optimization procedure will be illustrated with a plot in the *Harmonic fermions* title of Section 2.2.4 which is about the benchmark calculations.

2.1.3 Expectation value calculation

Expectation value calculation of the DMC should be modified in the correction scheme calculations. Necessary modifications are seen by integrating the eigenvalue equation (Eq. 1.2) over the simulation region volume Ω after the substitution of $\Phi(\mathbf{x}, \tau) + \Psi_T(\mathbf{x})$ for the wavefunction $\Psi(\mathbf{x})$:

$$\begin{aligned} E \int_{\Omega} [\Phi(\mathbf{x}, \tau) + \Psi_T(\mathbf{x})] d\Omega &= \int_{\Omega} \hat{H}_e [\Phi(\mathbf{x}, \tau) + \Psi_T(\mathbf{x})] d\Omega , \\ &= -\frac{1}{2} \int_{\Omega} \nabla^2 [\Phi(\mathbf{x}, \tau) + \Psi_T(\mathbf{x})] d\Omega \\ &+ \int_{\Omega} V(\mathbf{x}) [\Phi(\mathbf{x}, \tau) + \Psi_T(\mathbf{x})] d\Omega . \end{aligned} \quad (2.4)$$

Gathering the $\Psi_T(\mathbf{x})$ terms together allows a compact expression having $E_L(\mathbf{x})$. The kinetic energy term including $\Phi(\mathbf{x}, \tau)$ may be written as a surface integral using the divergence theorem in order to clarify its meaning. The final expectation value expression becomes [80]:

$$\langle E \rangle = \frac{-\frac{1}{2} \int_{\partial\Omega} \nabla \Phi(\mathbf{x}, \tau) \cdot d\mathbf{S} + \int_{\Omega} V(\mathbf{x}) \Phi(\mathbf{x}, \tau) d\Omega + \int_{\Omega} E_L(\mathbf{x}) \Psi_T(\mathbf{x}) d\Omega}{\int_{\Omega} \Phi(\mathbf{x}, \tau) d\Omega + \int_{\Omega} \Psi_T(\mathbf{x}) d\Omega} . \quad (2.5)$$

The first integral of the numerator in the above equation is about the walker flow at the boundaries of the simulation region which vanishes for the boson calculations being carried out in the all configuration space. For the fermion calculations in a nodal region or in a permutation cell, this term has a non vanishing contribution. The second integral of the numerator is the summation of walker potential energies in the expectation value calculation of the usual DMC. The last integral of the numerator is about the trial wavefunction being corrected which can be calculated in the beginning of the calculation without respecting the $\Psi_T(\mathbf{x})$ normalization using the Monte Carlo integration technique described in Section 1.2.2. The value of the $\Psi_T(\mathbf{x})$ integral of the denominator is given as a parameter of the method and it determines the

r_n parameter mentioned previously together with the number of walkers. Also, the value of the Monte Carlo integration calculated for the last term of the numerator is multiplied by this given value of the integral $\int_{\Omega} \Psi_T(\mathbf{x}) d\Omega$ for the omitted normalization issue. The remaining first integral of the denominator is just the number of walkers but it should be calculated as the difference of the numbers of the plus and minus signed walkers since the minus signed walkers are inherent in the correction scheme calculations due to the vacuum branchings.

The sum of the two integrals in the denominator of Eq. 2.5 may vanish causing problem in the energy calculation. This condition holds for fermions when the computation is carried out in a region where the antisymmetric wavefunction has equally positive and negative valued regions. Therefore, a suitable permutation cell which prevents this condition should be chosen for fermion systems. This issue applies to the calculation method discussed in Section 2.2 where appropriate permutation cells are chosen to prevent the mentioned problem.

2.2 Usage of the Correction Scheme in Non Fixed-Node DMC

The wavefunction correction technique described in the previous section is applied to the non fixed-node DMC as the main subject of this thesis study. The reduction of the statistical error in the non fixed-node DMC due to the correction scheme is investigated on some simple benchmark systems. The discussion of this section can also be found with a narrower context in the work of Dugan et al. [80].

The application of the wavefunction correction scheme to the non fixed-node DMC is similar to the boson case or the fixed-node fermion case. The fixed-node approximation is not facilitated for an exact treatment of the fermion nodes and some of the techniques described in Section 1.3 are used for increasing the stability of the calculations. Importance sampling is not facilitated in the benchmark calculations for better observing the sole effect of the correction scheme.

The computation region is restricted in a permutation cell as discussed in Section 1.3.5 and the outgoing walkers are permuted back with a sign inversion if an odd numbered permutations are applied. The permutation cell is chosen to be a positive valued nodal region of the trial wavefunction to avoid the problem mentioned in the last paragraph of the Section 2.1.3. The nodal regions of the trial wavefunctions should have permutation cell property for such

a choice to be valid and thus the trial wavefunctions are chosen considering this property in the benchmark computations. Minus signed walkers arise inevitably because of the vacuum branchings and the sign inversions at the permutation cell boundary. Therefore, the cancellation process of opposite signed walkers is facilitated in the correlated random walk process described in Section 1.3.3.

2.2.1 Algorithm details

- I *Initialization* : Equal amounts of plus and minus signed walkers are initialized in a positive valued permutation cell randomly or according to the trial wavefunction using the Metropolis algorithm.
- II *Diffusion* : Walker pairs are formed in each time step by finding the nearest unpaired minus signed neighbor of every plus signed walker. The plus signed walker takes a Gaussian random walk step according to Eq. 1.22 to simulate the effect of the diffusion kernel given in Eq. 1.20. The Gaussian random walk vector of the corresponding minus signed walker is found by reflecting the plus walker's Gaussian vector in the perpendicular bisector of the vector connecting the pair walkers.
- III *Cancellation* : Walker pairs are removed from the population when the Gaussian walk vectors of the pair members coincide in the diffusion step.
- IV *Branching* : Walkers of the both signs are subjected to the usual DMC branching according to Eq. 1.23 for simulating the effect of the branching kernel given in Eq. 1.21. When a minus signed walker reproduces in the branching process, the resulting new walker also has minus sign. The replication number n given in Eq. 1.24 does not exceed the upper limit 2 to avoid the branching instabilities.
- V *Vacuum Branchings* : Certain number of points are generated in the chosen permutation cell in each time step using the Metropolis algorithm according to the distribution $\Psi_T(\mathbf{x})$ which is positive definite in the simulation region. Extra branchings are carried out at these generated points with branching factors calculated linearly proportional to $[E_L(\mathbf{x}) - E_R]$.
- VI *Adjustment of the Reference Energy* : The DMC reference energy E_R is adjusted in each time step to keep the numbers of the plus and minus signed walkers equal to each other:

$$E_R = \langle E \rangle + \alpha \frac{N^+ - N^-}{\Delta\tau}, \quad (2.6)$$

where $\langle E \rangle$ is the calculated energy expectation value, α is a parameter which determines the strength of the adjustment and N^+ , N^- are the numbers of plus and minus signed walkers respectively.

VII *Expectation value Calculation* : The energy expectation value is calculated in each time step according to Eq. 2.5. The difference in the net number of walkers ($N^+ - N^-$) is calculated after the diffusion step for the flow term related to the surface integral and the other integrals are calculated as stated in Section 2.1.3. The cancellation process does not effect the net number of walkers since it eliminates one plus and one minus signed walker together.

The algorithm described above is applied for some time steps for thermalization and a time average of the expectation value is taken after the thermalization steps for desired number of time steps.

The method have been implemented using the object oriented *C++ programming language*. *GNU Scientific Library* (GSL) was used for the uniform and Gaussian random number generation processes. The implementation is distributed under *GNU Public License* (GPL) agreement and it can be requested from the current author.

2.2.2 Parameters

There are certain parameters of the method described in the previous subsection. Some of these parameters are inherited from the pure DMC method and there are two extra parameters necessary for the wavefunction correction scheme.

Parameters inherited from the pure DMC:

I *Time step interval* ($\Delta\tau$) : Determines the step size of the Gaussian random walk since it appears in the diffusion kernel (Eq. 1.20) and also affects the branching process according to Eq. 1.23. There is a time step error in the DMC method since it is devised for $\Delta\tau \rightarrow 0$ limit. Normally, a time step extrapolation is carried out after the DMC calculations

for some different values of $\Delta\tau$. However, in our benchmark calculations we omit this extrapolation step since the time step errors for the chosen values of $\Delta\tau$ are much smaller compared to the statistical error values.

- II *Thermalization and data collection steps* : Number of time steps for the thermalization and the data collection processes. The thermalization steps should be long enough to allow the walkers getting distributed according to the desired ground state wavefunction. The number of data collection steps should be determined according to the expected precision of the calculated expectation value result. It should be decided considering the fact that the statistical error value of the DMC run is inversely proportional to the square root of the number of data collection steps.
- III *Initial number of walkers (N^+, N^-)* : The numbers of plus and minus signed walkers initially created for the DMC run. The reference energy keeps N^+ and N^- equal to each other during the computation. However, these numbers may increase or decrease together, according to the cancellation rate of the opposite signed walkers.
- IV *E_R adjustment strength (α)* : Determines the strength of the reference energy adjustments. A small population control error arises if this parameter value is set to a very large value and large population fluctuations occur if its value is too small. This parameter value should be set to an intermediate value considering these problems associated with the two extremes.

Parameters for the correction scheme:

1. *Amplitude ratio (r_n)* : Ψ_T amplitude is defined as $\int \Psi_T(\mathbf{x}) d\Omega$ for which the trial wavefunction Ψ_T is positive in the simulation region Ω . The value of this integral is given as a parameter and it determines the ratio parameter r_n , described in Section 2.1.2, together with the stabilized value of the number of walker from each sign. Ψ_T amplitude value should be adjusted in such a way that the ratio r_n should have the largest value allowing a full correction of the trial wavefunction as discussed in Section 2.1.2 and analyzed in harmonic fermions benchmark calculations.
2. *Number of vacuum branching points (N^{vb})* : Determines the number of points generated using the Metropolis algorithm for the vacuum branching process. Exact value of this

parameter does not affect the computation significantly. Its value is taken equal to the initial number of walkers in the benchmark calculations.

2.2.3 Statistical error analysis

The expectation value for each benchmark system is calculated for certain times (n) using the methodology described in the previous subsections. The mean value \bar{E} of these separate calculation results are taken as the final expectation value:

$$\bar{E} = \frac{1}{n} \sum_{i=1}^n E_i, \quad (2.7)$$

where E_i are the individual calculation results. The statistical error of the mean is calculated using the formula:

$$\sigma = \sqrt{\frac{1}{n(n+1)} \sum_{i=1}^n (E_i - \bar{E})^2}. \quad (2.8)$$

The error calculated using the above formula is inversely proportional to the square root of the number of sample points n .

2.2.4 Benchmark computations

The method described in the previous subsections is applied to some simple systems for benchmarking. These calculation results are given below in separate titles.

Harmonic fermions

Harmonic fermions are preferred in the first application since their analytical solutions are known. Two fermion systems are studied for which the Hamiltonian function is as follows:

$$\hat{H} = -\frac{1}{2}(\nabla_1^2 + \nabla_2^2) + \frac{1}{2}\omega^2 (\mathbf{r}_1^2 + \mathbf{r}_2^2), \quad (2.9)$$

where ω is a constant which has the numerical value of 0.03 in the all calculations and $\mathbf{r}_1, \mathbf{r}_2$ are the position vectors of the two fermions.

The trial wavefunctions used in the correction process are chosen as

$$\Psi_T = e^{\varepsilon_1 \frac{\omega}{2} (\mathbf{r}_1^2 + \mathbf{r}_2^2)} (x_2 + \varepsilon_2 y_2^2 - x_1 - \varepsilon_2 y_1^2), \quad (2.10)$$

where x, y are the particle coordinate components in two separate space dimensions and $\varepsilon_1, \varepsilon_2$ are free parameters. This function gives the true antisymmetric ground state for the used Hamiltonian function in $\varepsilon_1 \rightarrow 1, \varepsilon_2 \rightarrow 0$ limit, regardless of the number of space dimensions (number of dimensions in which the fermions make harmonic oscillation). The parameter ε_1 is used to distort the exponential function in Ψ_T and the parameter ε_2 is used to distort the nodal hyper surface, preserving the permutation cell property of the nodal region. Such a node distortion is not possible when there is only one space dimension in the harmonic fermions system studied. A positive valued nodal region of the trial wavefunction is chosen as the simulation region to avoid the instability due to the denominator of the expectation value expression Eq. 2.5. The outgoing walkers are permuted back to inside with a sign inversion when necessary.

Harmonic fermion calculations are carried out for up to 4 space dimensions. The parameter values discussed in the Section 2.2.2 are adjusted suitably considering the guidelines given in that section. Value of the time step parameter $\Delta\tau$ is set to 0.003 in dimensionless units. 6000 time steps are taken for the thermalization and the data is collected for 5000 time steps. The computation for each case is carried out for 16 different seeds of the random number generator for calculating the mean and the statistical error as described in Section 2.2.3. DMC simulations are initialized with 500 walkers from each sign and the stabilized values of population sizes are given for each space dimension in Table 2.1 which shows the computation results for harmonic fermions. The reference energy adjustment parameter α is given the value 0.00001. The amplitude ratio parameter (r_n) values are adjusted to have optimum values for each computation separately. N^{vb} , the number of points for the vacuum branchings are set to the constant value of 500 as the initial number of walkers from each sign.

Computations are also carried out without using the correction scheme for a comparison of the computational efforts of the two cases. DMC without any corrected trial wavefunctions

is used for these comparison calculations. Same permutation cells that used in the correction scheme computations are used where outgoing walkers are treated in the same way. Correlated walk of opposite signed walkers with the cancellation process is also facilitated in the comparison case computations. Computation times of the two cases for calculating the results with certain statistical error values are compared. The accuracies of the two cases are the same since neither of the methods have any systematic error other than the time step error. The implementations and the used external libraries are also the same for the two cases except the wavefunction correction related parts which do not exist in the comparison case calculations. Therefore, the computation time to achieve a certain precision is a reasonable comparison issue.

Computation results for the correction scheme harmonic fermion calculations (E_c) are given in Table 2.1 together with the comparison of the computation times with the usual DMC computations (r_t). Efficiency improvements can be seen from these r_t ratios of the comparison case computation times to the correction scheme computation times. Significant decreases in the computation times are observed for the all studied space dimensions when the correction scheme is used.

Table 2.1: Correction scheme computation results for two harmonic fermions. d : space dimension, $\varepsilon_1, \varepsilon_2$: disturbance parameter values, E_c : calculated energy expectation value using the correction scheme, E_{GS} : true value of the fermionic ground state energy, E_T : trial wavefunction energy (all energies are given in dimensionless units), N_w : stabilized number of walkers from each sign, r_n : ratio of the trial wavefunction normalization to the number of walkers from each sign, r_t : ratio of the comparison case computation time to the correction scheme computation time.

d	ε_1	ε_2	E_c	E_{GS}	E_T	N_w	r_n	r_t
1	0.964	0.00	0.34644(31)	0.34641	0.34677	195	14.4	2.7
2	1.000	0.05	0.51978(62)	0.51962	0.52205	495	5.7	5.5
3	1.000	0.05	0.6932(11)	0.69282	0.70143	520	4.6	8.8
4	1.000	0.05	0.8660(10)	0.86603	0.87473	1556	1.9	4.8

Images for the trial wavefunction (top image) and its difference from the true fermionic wavefunction (middle image) is given in Figure 2.2 for the 1D computation whose configuration space is two dimensional. Average walker distribution during the correction scheme DMC computation (bottom image) is also given. Walker distribution is calculated in a single per-

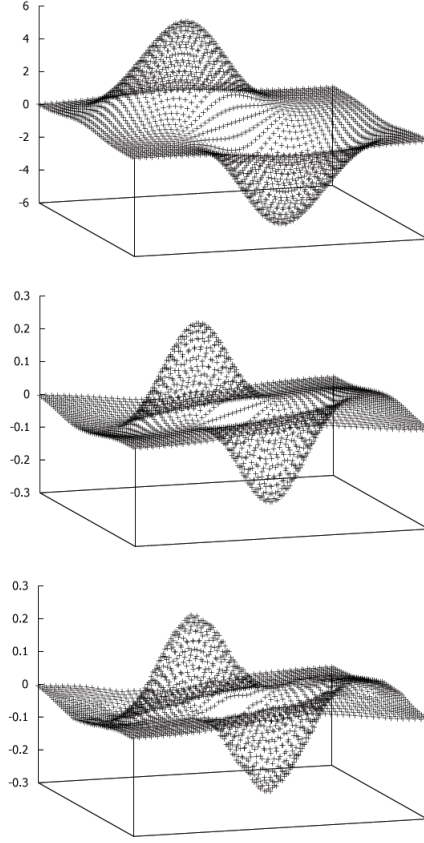


Figure 2.2: Wavefunction plots for correction scheme DMC computation of the two harmonic fermions in 1D. **TOP:** Trial wavefunction. **MIDDLE:** Difference between the true fermionic ground state and the trial wavefunction. **BOTTOM:** Average walker distribution during the DMC computation.

mutation cell and it is reflected to the other cell with a sign inversion in order to generate a plot for the all configuration space. Minus signed walkers give negative weights when the average is calculated. Walker distribution fits well with the difference function as expected when the correction scheme is used.

The effect of the amplitude ratio parameter (r_n) on the statistical error values and also on the computation results are investigated by doing the 1D harmonic fermion calculation with various values of this parameter. These computation results are plotted in Figure 2.3 to give an intuition about the optimization procedure of the parameter r_n . The statistical error decreases as expected when the r_n value increases. The calculated energy expectation value fluctuates around the true value until the r_n value of 14.4 and a deviation from the true value occurs after this point which is chosen as the optimum value of the r_n parameter.

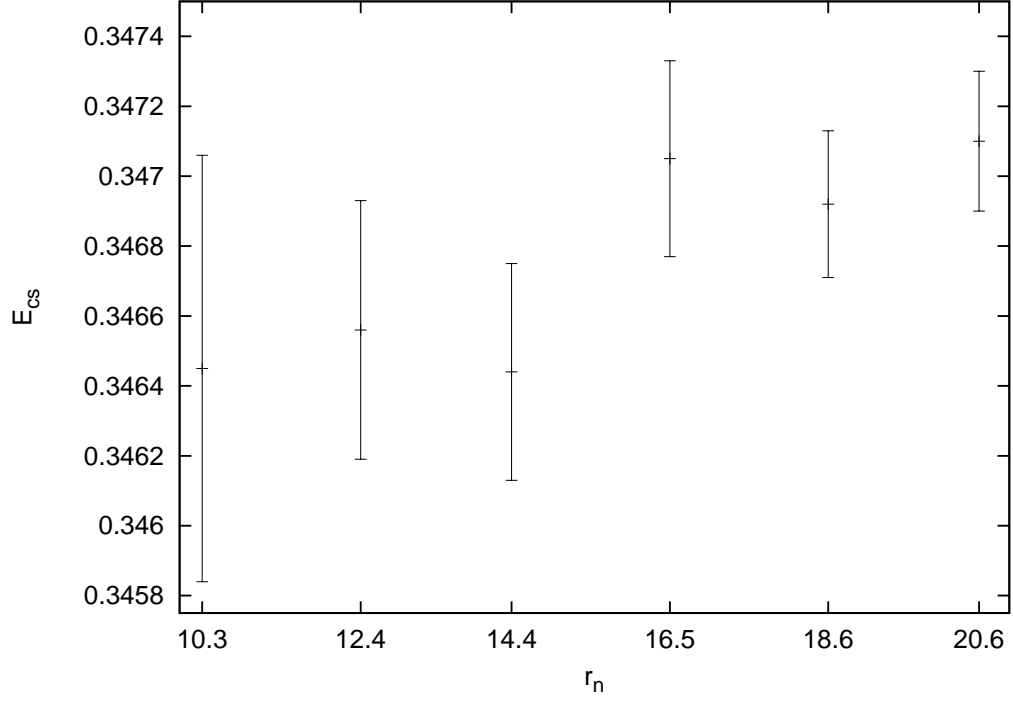


Figure 2.3: Calculated energy expectation value versus normalization ratio parameter r_n for harmonic fermions in 1D.

Helium atom lowest triplet state

As a physical example, the wavefunction correction technique is used to calculate the non-relativistic energy expectation value of the lowest triplet state of the Helium atom ($1s2s\ ^3S$) without using the fixed-node constraint. This particular state is chosen since it has antisymmetric spatial wavefunction causing the sign problem. The electronic Hamiltonian function (Eq. 1.8) is used and the trial wavefunction is chosen as a Slater determinant taken from the work of Emmanouilidou et al. [81]:

$$\Psi_T = e^{-(2r_1 + \alpha r_2)}(1 - \alpha r_2) - e^{-(2r_2 + \alpha r_1)}(1 - \alpha r_1), \quad (2.11)$$

where r_1 and r_2 are the electron nucleus distances for the two electrons of the system and the numerical value of the parameter α is chosen as 0.65.

The nodal surface of the studied state of the Helium atom is well known as $r_1 = r_2$ surface [45] which does not match with the nodal surface of the trial wavefunction (Eq. 2.11) used in

the calculation. Trial wavefunction cross section is plotted in Figure 2.4 for $r_1 = 2 r_2$ surface. A node crossing is seen in this plot proving that the nodal surface of Eq. 2.11 extends out of the true nodal surface. Such node crossings always exist for the surfaces $r_1 = k r_2$ with positive k values.

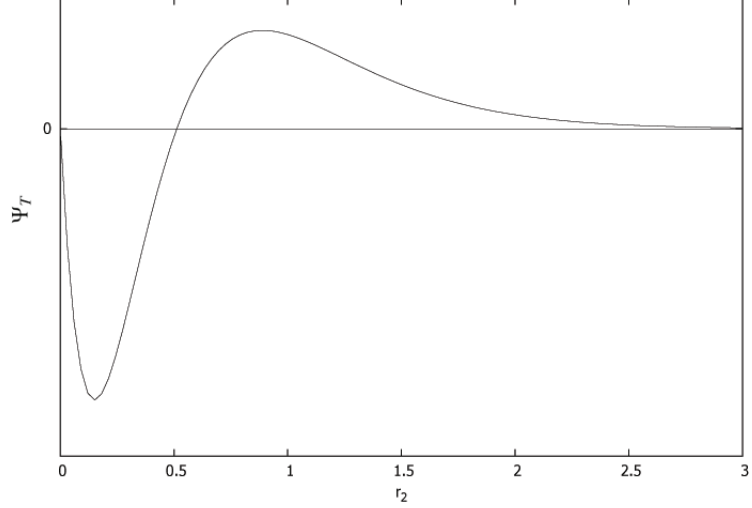


Figure 2.4: He atom $1s2s\ ^3S$ state trial wavefunction (Eq. 2.11) cross section on $r_1 = 2 r_2$ surface. Node crossing is seen at $r_2 = 0.5$ a.u.

DMC time step $\Delta\tau$ is chosen as 0.0005 atomic time units and the data is collected for 80000 time steps after 6000 thermalization steps. Initial number of plus and minus signed walkers and the number of points for the vacuum branchings are set to 500. The reference energy adjustment parameter is chosen as 2×10^{-6} . The amplitude of the trial wavefunction is set to 2600 and the number of walkers of each sign is stabilized around 520, giving the r_n value as 5.0.

The non-relativistic true energy expectation value for this state is -2.1752 Hartrees [82] and the energy expectation value of the used trial wavefunction is -2.1548 Hartrees. Current correction scheme calculation gives the result as -2.1767(63) Hartrees for which the true value is in the statistical error interval. Same kind of comparison is made for the He atom as in the case of the harmonic fermions and the computation time of the correction scheme calculation is 4.2 times shorter than the computation time to achieve the same precision with the comparison case calculation without any trial wavefunctions. Fixed-node DMC calculation using the nodes of the used trial wavefunction gives the energy value as -2.1626(8) Hartrees confirming the deviation of the trial wavefunction nodal surface from the true nodal surface $r_1 = r_2$.

Hydrogen molecule

The last computation used for benchmarking is carried out for the Hydrogen molecule. As in the case of the helium atom, the lowest lying state with antisymmetric spatial wavefunction is studied. In fact, this state of the Hydrogen molecule is not a bound state since there is a repulsive force between the two nuclei for all separation distances d . However, a single point energy calculation can still be carried out for a chosen separation of the nuclei which was chosen as $d = 3.0$ a.u. in the current calculation.

The trial wavefunction is chosen as a Slater determinant formed by the hydrogenic ground state orbitals around the two nuclei:

$$\Psi_T = e^{-(r_{11}+r_{22})/d} - e^{-(r_{12}+r_{21})/d}, \quad (2.12)$$

where r_{ij} denote distances between i th electron and j th nucleus. The energy expectation value of this trial wavefunction is calculated as -0.9646 Hartrees using Monte Carlo integration technique. $\Delta\tau$, thermalization steps and data collection steps parameter values are chosen as the same values as the He atom calculation case. Initial number of walkers from each sign (N^+, N^-) and the parameter N^{vb} are set to 400. Ψ_T amplitude is set to 2000 and the population sizes are stabilized around 437 giving an r_n value of 4.6. The energy expectation value for the studied state is calculated as $-0.9699(38)$ Hartrees using the non fixed-node correction scheme DMC which is slightly lower than the trial wavefunction energy. The computation time is roughly 33 minutes which is 3.5 times shorter than the computation using the non fixed-node calculation without wavefunction correction technique to achieve the same precision.

2.2.5 Discussion about the benchmark calculation results

Application of the wavefunction correction scheme to the non fixed-node DMC reduces the statistical error of the method significantly. Benchmark computations on the harmonic fermions, helium atom and the hydrogen molecule show that the computation time for calculating the result within a certain statistical error value decreases several times when the correction scheme is used. Improvement of the precision depends on the ratio of the trial wavefunction ampli-

tude to the number of walkers and this parameter of the method can be increased when the trial wavefunction gets closer to the true fermionic wavefunction. Therefore, quality of the trial wavefunction is an important factor affecting the precision improvements observed in the correction scheme calculations. The mentioned ratio parameter value should be set to the highest value allowing a full correction which can be guessed considering the quality of the trial wavefunction. This parameter value can be optimized using the fact that a deviation in the calculated expectation value starts to occur beyond the optimum value of the parameter.

The nodal surfaces of the used trial wavefunctions deviate from the true surfaces for the all cases except the harmonic fermions calculation in 1D for which a permutation cell preserving node distortion is not possible. The correction scheme calculations yield the true energy expectation value despite the wrong nodal surfaces which proves the applicability of the wavefunction correction scheme for the non fixed-node QMC calculations. This discussion does not apply to the hydrogen molecule calculation for which the true value of the calculated state is not available.

The fixed-node DMC is applicable to large systems since it eliminates the minus signed walkers by constraining the computation in a nodal region. This advantage of the fixed-node approximation disappears with the usage of the correction scheme because of the arising minus signed walkers as a result of the vacuum branchings. However, the wavefunction correction technique is suitable for non fixed-node DMC computations since the minus signed walkers are already needed for plus-minus cancellation methods. Correction scheme improves the large scale applicability for such calculations as opposed to the case for the fixed-node calculations.

Benchmark computations are carried out without using the importance sampling transformation in order to better observe the sole effect of the wavefunction correction technique. Importance sampling may be facilitated in the correction scheme calculations as described in the references [78, 79]. However, the guiding function should allow the walkers' passage from the boundaries of the chosen permutation cell for the application of the current boundary conditions when the fixed-node constraint is relaxed. A slightly modified form of the corrected trial wavefunction which does not vanish on the nodal surface of the original function may be used as the guiding function.

2.3 Stable Non Fixed-Node Algorithm Using Correction Scheme

Some modifications on the wavefunction correction scheme are discussed in this section towards the development of a DMC algorithm which does not suffer from the instabilities due to the fermion sign problem. These developments do not resolve the sign problem but they serve as a different viewpoint towards the solution and understanding the nature of the problem.

2.3.1 Downwards shift of the trial wavefunction

In the original form of the wavefunction correction scheme, the trial wavefunction is corrected both in the positive and negative directions depending on the sign of the difference $\Psi_{GS}(\mathbf{x}) - \Psi_T(\mathbf{x})$. Therefore, minus signed walkers are indispensable for the correction process in the negative direction. Negative directional corrections can be avoided by a certain amount downwards shifting of the trial wavefunction $\Psi_T(\mathbf{x})$ which is illustrated in Figure 2.5.

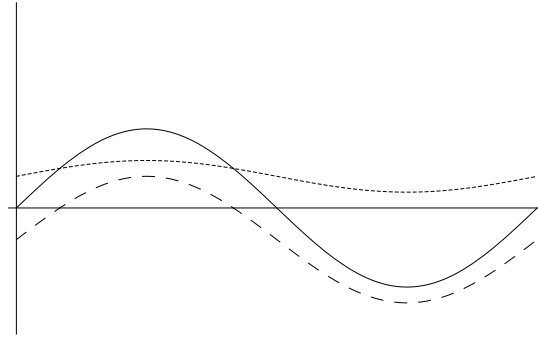


Figure 2.5: Downwards shift of the trial wavefunction $\Psi_T(\mathbf{x})$. **Dashed Line:** Shifted trial wavefunction $\Psi_T^s(\mathbf{x})$, **Solid Line:** Ground state wavefunction $\Psi_{GS}(\mathbf{x})$, **Dotted Line:** Difference function $\Psi_{GS}(\mathbf{x}) - \Psi_T^s(\mathbf{x})$.

The difference function $\Psi_{GS}(\mathbf{x}) - \Psi_T^s(\mathbf{x})$ becomes positive definite as seen in the figure if the shift amount is sufficient. Necessary shift amount for having a positive definite difference function reduces as the quality of the trial wavefunction increases.

The shifting of the trial wavefunction may be position dependent using a shift function $S(\mathbf{x})$:

$$\Psi_T^s(\mathbf{x}) = \Psi_T(\mathbf{x}) - S(\mathbf{x}) . \quad (2.13)$$

A position dependent shift is advantageous compared to a constant shift as $\Psi_T(\mathbf{x}) - c$, since the irrelevant vanishing parts of the trial wavefunction are also shifted in the constant shift case. Those irrelevant parts are not altered when the shift function is chosen as:

$$S(\mathbf{x}) = \sqrt{a \exp(-b d^2) + \Psi_T^2(\mathbf{x})}, \quad (2.14)$$

where a and b are adjustable parameters. Ψ_T^2 term causes a downwards shift proportional to the magnitude of the trial wavefunction and the exponential factor is necessary to avoid the negative directional corrections about the approximate nodal surface. The variable d should reflect in some manner, the distance of the vector \mathbf{x} from the approximate nodal surface of Ψ_T .

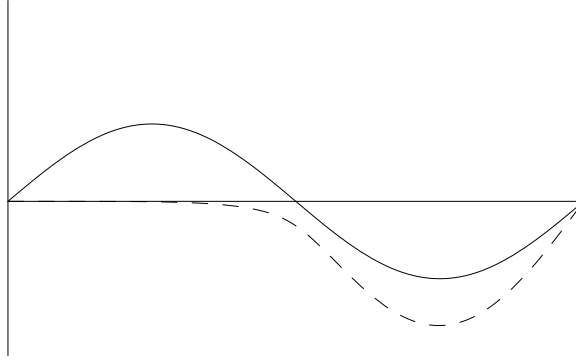


Figure 2.6: Position dependent shift of the trial wavefunction. **Dashed Line:** Shifted trial wavefunction $\Psi_T^s(\mathbf{x})$, **Solid Line:** Ground state wavefunction $\Psi_{GS}(\mathbf{x})$.

In Figure 2.6, a trial wavefunction with such a position dependent shift is plotted together with the ground state wavefunction. The difference $\Psi_{GS}(\mathbf{x}) - \Psi_T^s(\mathbf{x})$ is positive definite and the irrelevant parts of the trial wavefunction are not shifted as seen in the figure.

2.3.2 Vacuum branchings at walker positions

The minus signed walkers still arise due to the vacuum branching process described in the Section 2.1.1 despite the downwards shifting of the trial wavefunction to avoid the negative directional corrections. However, the minus signed walkers may be avoided in the vacuum branching process if these extra branchings are carried out at the walker positions instead of the random points generated according to the trial wavefunction using the Metropolis algo-

rithm. Instead of creating a minus signed walker, the walker on which the extra branching is being made is killed in this case. The branching factors for such an application are calculated as:

$$W(\mathbf{x}) = 1 - [E_L(\mathbf{x}) - E_R]\Delta\tau \Psi_T^s(\mathbf{x})/D_w(\mathbf{x}, \tau) . \quad (2.15)$$

The rescaling factor $\Psi_T^s(\mathbf{x})/D_w(\mathbf{x}, \tau)$ is necessary since the extra branchings are carried out according to a distribution other than the trial wavefunction $\Psi_T^s(\mathbf{x})$. The division factor $D_w(\mathbf{x}, \tau)$ is the instantaneous value of the walker distribution at the position of the branching which can be calculated as a *density of walkers* calculation at the close neighborhood of the branching position. The density of walkers calculation is carried out as counting the walkers in a certain cubical box having the same dimensionality as the configuration space, centered at the branching position. This density measure works very well for small dimensional configuration spaces and it enables the vacuum branchings to be carried out without any need for the minus signed walkers. However, as the dimensionality of the configuration space increases, the dimensions of the box in which the walkers are counted should also increase in order to have a non vanishing probability of some walkers being counted in the box. For relatively large systems, the dimensions of the box becomes comparable to the dimensions of the relevant configuration space where the physical wavefunction has significantly non zero values and the density measure consequently becomes imprecise. For better describing the problem about the mentioned density measure, the formula for the length of a dimension of the chosen box (l_{box}) is given below to have a volume which is 1/1000 of the volume of the relevant configuration space which is assumed to be box shaped for convenience:

$$l_{box} = \frac{l}{\sqrt[d \times n]{1000}} , \quad (2.16)$$

where l is the length of a dimension of the relevant configuration space. As an example, the numerical value of the ratio l_{box}/l becomes 0.9332 when the configuration space dimension ($d \times n$) is 100.

An alternative density calculation technique, which would better work for higher dimensional configuration spaces, is to use the average distance between certain number of walkers in the close neighborhood of the branching position. However, tests with such a density mea-

sure shows that it does not give results with sufficient precision even for small systems and therefore not suitable.

The mentioned problem about the density measure is indeed originated from the fact that the walker distribution becomes very sparse as the dimensionality of the configuration space increases. The sparsity of the walker distribution, therefore, avoids the large scale applicability of the stable method described in this section.

2.3.3 Two permutation cells and two reference energies

A technique to avoid the minus signed walkers in the vacuum branching process was discussed in the previous subsection. However, the minus signed walkers arise also due to the sign inversions at the permutation cell boundaries as described in Section 1.3.5. These sign inversions are avoided by making the calculation in two permutation cells (instead of a single permutation cell) related to each other with a single permutation of identical particles (or any odd numbered permutations). When such a simulation region is chosen, all the outgoing walkers are taken inside by the appropriate particle permutations without any sign inversions. However, the antisymmetry condition of the fermionic wavefunction in this case should be imposed in a different manner since the avoided process of sign inversions at the permutation cell boundaries had previously served for the antisymmetry imposition in the method described in Section 2.2.

The antisymmetry is imposed in the two permutation cells calculation by normalizing the wavefunction separately in the two cells using two reference energies. The sums $\int \Psi_T^s(\mathbf{x}) d\Omega_1 + N_1$ and $\int \Psi_T^s(\mathbf{x}) d\Omega_2 + N_2$ are kept constant at different values (The normalization value in the second cell is the multiplication inverse of the normalization value in the first cell as required by the antisymmetry.) in the two cells via adjustments of the reference energies E_R^1, E_R^2 separately. N_1 and N_2 in the above expressions denote the number of walkers in the first and second cells respectively. These walkers have all plus signs since the minus signed walkers are avoided with the techniques described in the previous and current subsections.

Using two separate reference energies in the two cells corresponds to introducing a position dependent reference energy $E_R(\mathbf{x})$ in Eq. 1.16. Therefore, the stable method described in this section is not exact even if an accurate density measure could have been devised for

the application of the vacuum branchings at walker positions as described in the previous subsection.

2.3.4 Harmonic fermion calculations using the stable algorithm

The stable DMC algorithm described in previous subsections is used to calculate the ground state eigenvalues of the harmonic fermions discussed in Section 2.2.4. The purpose of these calculations is to test the effects of the density measure and the usage of two reference energies on the accuracy of the results. Trial wavefunction given in Eq. 2.10 is used as Ψ_T also in these calculations. Ψ_T^s is generated according to the formula given in Eq. 2.13 using the shift function $S(\mathbf{x})$ of Eq. 2.14.

The calculation is initially carried out for one space dimension to test the effect of two reference energy usage. The density measure as counting the walkers in a certain cubical box is accurate enough for such a small dimensional system and thus the sole effect of the two reference energies is tested with this 1D calculation. The disturbance parameters ε_1 and ε_2 of the trial wavefunction (Eq. 2.10) are given the values 0.9238 and 0.0 respectively. The parameters a and b of the shift function $S(\mathbf{x})$ are set to the values 1.0 and 0.1 respectively. The distance d in $S(\mathbf{x})$ expression is measured from the origin of the coordinate system. $\Delta\tau$ is set to 0.001 and α is set to 0.00001. The numbers of walkers in each cell is kept constant at 500 and the values of $\int \Psi_T^s(\mathbf{x}) d\Omega$ integrals are given the values -83.6 and -916.4 in the two cells to satisfy the antisymmetry condition of the wavefunction. The length of a dimension of the cubical box is set to 0.77 dimensionless units (d.u.) for the density of walkers calculation. The ground state energy eigenvalue is calculated as 0.3465(11) d.u. using the stable correction scheme DMC algorithm with shifted trial wavefunction in 280000 time steps. The calculated value is very close to the true value which is 0.34641 d.u. for the 1D harmonic fermions (see Table 2.1). The values of the two reference energies deviate from each other significantly during the computation. However, the time averages of them are 0.34892 and 0.35179 d.u. for E_R^1 and E_R^2 which are close to each other. Therefore, two reference energy usage does not cause a significant bias for the 1D calculation. Average walker distribution during this computation is compared with the expected walker distribution ($\Psi_{GS} - \Psi_T^s$) in Figure 2.7. The comparison shows that the shape of the walker distribution fits with the expected distribution in general. However, it is not as accurate as the calculation results of Section 2.2 which was

plotted in Figure 2.2.

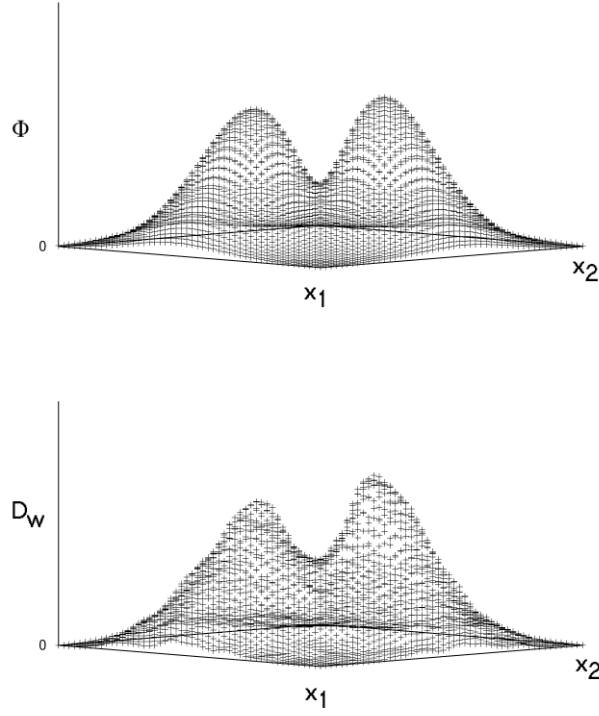


Figure 2.7: Wavefunction plots for two harmonic fermions in 1D. Horizontal axes x_1 , x_2 are the positions of the two fermions. **TOP:** Difference between the true fermionic ground state and the shifted trial wavefunction ($\Phi = \Psi_{GS} - \Psi_T^s$). **BOTTOM:** Average walker distribution during the DMC computation (D_w).

As the next step, the harmonic fermion calculation is repeated in 10 space dimensions (20 dimensional configuration space) in order to test the accuracy reductions due to the density measure in higher dimensional configuration spaces. The value of the parameter a of $S(\mathbf{x})$ function is reduced to 0.001 since a larger value is not suitable for such a high dimensional configuration space. The length of a dimension of the cubical box is set to 10.47 d.u. in the density of walkers calculation, to keep the walker counting probability the same as the 1D case. This length value for a dimension of the cubical box is very large since the relevant configuration space dimension is about 14 d.u. Therefore, a precise density of walkers calculation is not expected. All the other parameters have the same values as in the case of the 1D calculation. The ground state eigenvalue is computed as 1.9185(34) in 80000 time steps using the algorithm described in this section. There was no instability problem during

the calculation of this higher dimensional system. However, the accuracy of the result is not very good since it deviates from the true value which is 1.9053 for the studied two harmonic fermions in 10D. This bias in the calculated result is expected since the density measure was very imprecise for this higher dimensional calculation.

CHAPTER 3

CONCLUSIONS

Some developments on the DMC method, which is used to find the ground state solutions of the Schrödinger equation, are discussed in this thesis work. The context of the developments is divided in to two parts both related to the wavefunction correction scheme DMC calculations:

The first part of the developments (Section 2.2) are about the application of the wavefunction correction scheme to the non fixed-node DMC in order to reduce the statistical error bars obtained in a certain amount of computation time. The non fixed-node DMC method used in the calculations does not have the nodal systematic error encountered in the fixed-node DMC calculations. However, it is unstable due to the fermion sign problem and consequently its application to relatively large systems is not possible. The developments of the first part does not affect the stability of the non fixed-node DMC but they are aimed to shorten the computation times of the non fixed-node calculations in their current application range. The benchmark computation results indicate that computation times to achieve a certain precision decreases several times when the correction scheme is used in the non fixed-node DMC. Therefore, the objective of the developments of the first part is achieved successfully. Also, it should be noted that, the wavefunction correction technique introduces minus signed walkers to the boson and fixed-node fermion calculations and thus it reduces the stability of such DMC calculations. This problem does not arise in the non fixed-node DMC framework since the minus signed walkers and the instability are already inherit in such calculations.

In the second part of the developments, discussed in Section 2.3, some modifications on the original wavefunction correction scheme are studied with a purpose of having a stable non fixed-node DMC algorithm. These developments avoid the minus signed walkers in such calculations by converting the plus - minus cancellation process in to a density of walkers

calculation. Both of these processes suffer from the sparsity of the walker population in higher dimensional configuration spaces when relatively larger systems are considered. The necessity for the density of walkers calculation in the new developments reduces the accuracy of the DMC calculations, especially for large systems, since an accurate density calculation is not possible for a very sparse walker distribution. However, the developed method is stable and it is useful for understanding the nature of the fermion sign problem. Since a sparse walker distribution is the main cause of the problem in the new developed method as in the case of the plus - minus cancellation methods, it becomes apparent that an exact fermion calculation is not possible in the DMC framework without fully generating the wavefunction. In other words, the statistical sampling techniques, which are very successful for boson calculations, become inefficient when the antisymmetry condition of the fermions is desired to be imposed on the wavefunction exactly.

REFERENCES

- [1] K. Raghavachari. Electron correlation techniques in quantum chemistry: Recent advances. *Annu. Rev. Phys. Chem.*, 42:615–42, 1991.
- [2] R. J. Bartlett and M. Musia. Coupled-cluster theory in quantum chemistry. *Rev. Mod. Phys.*, 79:291–352, 2007.
- [3] S. Goedecker. Linear scaling electronic structure methods. *Rev. Mod. Phys.*, 71:1085–1123, 1999.
- [4] G. E. Scuseria. Linear scaling density functional calculations with gaussian orbitals. *J. Phys. Chem. A*, 103:4782–4790, 1999.
- [5] P. Hohenberg and W. Kohn. Inhomogeneous electron gas. *Phys. Rev.*, 136:B864–B871, 1964.
- [6] M. Springborg. *Methods of Electronic-Structure Calculations*. John Wiley and Sons Ltd., 2000.
- [7] W. A. Lester A. Aspuru-Guzik. Quantum Monte Carlo methods for the solution of the Schrödinger equation for molecular systems. *arXiv: cond-mat*, 0204486, 2002.
- [8] W. M. C. Foulkes, L. Mitas, R. J. Needs, and G. Rajagopal. Quantum Monte Carlo simulations of solids. *Rev. Mod. Phys.*, 73:33–83, 2001.
- [9] P. Echenique and J. L. Alonso. A mathematical and computational review of Hartree-Fock SCF methods in quantum chemistry. *Molecular Physics*, 105:3057–3098, 2007.
- [10] J. B. Anderson. Quantum chemistry by random walk. $\text{H}_3^+ D_{3h}^+ {}^1A_1$, $\text{H}_2 {}^3\Sigma_u^+$, $\text{H}_4 {}^1\Sigma_g^+$, $\text{Be } {}^1S$. *J. Chem. Phys.*, 65:4121–4127, 1976.
- [11] R. Shankar. *Principles of Quantum Mechanics, 2nd Edition*. Plenum Press, New York, 1994.
- [12] J. J. Sakurai. *Modern Quantum Mechanics, Rev. ed.* Addison Wesley, 1994.
- [13] E. Schrodinger. Quantisierung als eigenwertproblem. *Annalen der Physik. Leipzig*, 79:489–527, 1926.
- [14] H. P. Stapp. The Copenhagen interpretation. *Am. J. Phys.*, 40:1098–1116, 1972.
- [15] A. Whitaker. *Einstein, Bohr and the quantum dilemma*. Cambridge University Press, New york, 1996.
- [16] J. D. Walecka. *Fundamentals of Statistical Mechanics*. Imperial College Press, World Scientific, Singapore, 2000.
- [17] I. Duck and E. C. G. Sudarshan. Toward an understanding of the spin-statistics theorem. *Am. J. Phys.*, 66:284–303, 1998.

- [18] H. C. Ohanian. What is spin. *Am. J. Phys.*, 54:500–505, 1986.
- [19] M. Born and R. Oppenheimer. Zur quantentheorie der moleküle. *Annalen der Physik. Leipzig*, 84:457–484, 1927.
- [20] A. J. James. *Solving the Many Electron Problem with Quantum Monte-Carlo Methods*. PhD thesis, Imperial College of Science, 1995.
- [21] I. Kosztin, B. Faber, and K. Schulten. Introduction to the diffusion Monte Carlo method. *Am. J. Phys.*, 64:633–646, 1996.
- [22] N. Metropolis. The beginning of the Monte Carlo method. *Los Alamos Science*, Special Issue:125–130, 1987.
- [23] W. A. Lester, L. Mitas, and B. Hammond. Quantum Monte Carlo for atoms, molecules and solids. *Chem. Phys. Lett.*, 478:1–10, 2009.
- [24] R. J. Needs, M. D. Towler, N. D. Drummond, and P. L. Rios. Continuum variational and diffusion quantum Monte Carlo calculations. *J. Phys.: Condens. Matter*, 22:023201–15, 2010.
- [25] H. G. Evertz and M. Marcu. *Quantum Monte Carlo methods in condensed matter physics*, ed. M. Suzuki. World Scientific, Singapore, 1993.
- [26] J. Shumway and D. M. Ceperley. *Quantum Monte Carlo Methods in the Study of Nanostructures in Handbook of Theoretical and Computational Nanotechnology*, eds. M. Rieth and W. Schommers, *Encyclopedia of Nanoscience and Nanotechnology*, Vol. 3. American Scientific Publishers, 2006.
- [27] J. B. Anderson. *Quantum Monte Carlo: Origins, Development, Applications*. Oxford University Press, New york, 2007.
- [28] R. N. Barnett and K. B. Whaley. Variational and diffusion Monte Carlo techniques for quantum clusters. *Phys. Rev. A*, 47:4082–4098, 1993.
- [29] S. A. Alexander and R. L. Coldwell. Calculating atomic properties using variational Monte Carlo. *J. Chem. Phys.*, 103:2572–2575, 1995.
- [30] N. A. Benedek, I. K. Snooka, M. D. Towler, and R. J. Needs. Quantum Monte Carlo calculations of the dissociation energy of the water dimer. *J. Chem. Phys.*, 125:104302–5, 2006.
- [31] M. H. Kalos. Monte Carlo calculations of the ground state of three- and four-body nuclei. *Phys. Rev.*, 128:1791–1795, 1962.
- [32] D. M. Ceperley. Metropolis methods for quantum Monte Carlo simulations. *arXiv:physics*, 0306182, 2003.
- [33] M. Lewerenz. Monte Carlo methods: Overview and basics. *NIC Series*, 10:1–24, 2002.
- [34] R. H. Landau, M. J. Paez, and C. C. Bordeianu. *Computational Physics: Problem Solving with Computers*. WILEY-VCH, 2007.
- [35] N. Metropolis, A. Rosenbluth, M. Rosenbluth, A. Teller, and E. Teller. Equation of state calculations by fast computing machines. *J. Chem. Phys.*, 21:1087–000, 1953.

- [36] E. Polak. *Optimization : Algorithms and Consistent Approximations*. Springer, New York, 1997.
- [37] P. Ballone and P. Milani. Simulated annealing of carbon clusters. *Phys. Rev. B*, 42:3201–3204, 1990.
- [38] S. Forrest. Genetic algorithms: Principles of natural selection applied to computation. *Science*, 261:872–878, 1993.
- [39] J. C. Slater. Theory of complex spectra. *Phys. Rev.*, 34:293–1322, 1929.
- [40] D. Ceperley. *Solving quantum many-body problems with random walks*. Computational Physics, Proceedings of Ninth Physics Summer School, Australian National University, 1997.
- [41] G Ortiz, D. M. Ceperley, and R. M. Martin. New stochastic method for systems with broken time-reversal symmetry; 2-D fermions in a magnetic field. *Phys. Rev. Lett.*, 71:2777–0000, 1993.
- [42] R.C. Grimm and R.G. Storer. Monte Carlo solution of Schrodinger’s equation. *J. Comput. Phys.*, 7:134–156, 1971.
- [43] R. Assaraf, M. Caffarel, and A. Khelif. The fermion Monte Carlo revisited. *J. Phys. A: Math. Theor.*, 40:1181–1214, 2007.
- [44] M. Troyer and U. J. Wiese. Computational complexity and fundamental limitations to fermionic quantum Monte Carlo simulations. *Phys. Rev. Lett.*, 94:170201–170204, 2005.
- [45] D. Bressanini, D. M. Ceperley, and P. J. Reynolds. What do we know about wave function nodes? *arXiv:quant-ph*, 0106062, 2001.
- [46] M. Bajdich, L. Mitas, G. Drobný, and L. K. Wagner. Approximate and exact nodes of fermionic wavefunctions: Coordinate transformations and topologies. *Phys. Rev. B*, 72:075131–5, 2005.
- [47] S. Manten and A. Luchow. On the accuracy of the fixed-node diffusion quantum Monte Carlo method. *J. Chem. Phys.*, 115:5362–5366, 2001.
- [48] J. C. Grossman and L. Mitas. Quantum Monte Carlo determination of electronic and structural properties of Si_n clusters ($n \leq 20$). *Phys. Rev. Lett.*, 74:1323–1326, 1995.
- [49] W. A. Lester and R. Salomon-Ferrer. Some recent developments in quantum Monte Carlo for electronic structure: Methods and application to a bio system. *J. Mol. Struct.: THEOCHEM*, 771:51–54, 2006.
- [50] E. Sola, J. P. Brodholt, and D. Alfe. Equation of state of hexagonal closed packed iron under earths core conditions from quantum Monte Carlo calculations. *Phys. Rev. B*, 79:024127–6, 2009.
- [51] S. Bovino, E. Coccia, E. Bodo, D. Lopez-Duran, and F. A. Gianturco. Spin-driven structural effects in alkali doped ^4He clusters from quantum calculations. *J. Chem. Phys.*, 130:224903–9, 2009.

- [52] G. Rajagopal, R. J. Needs, A. James, S. D. Kenny, and W. M. C. Foulkes. Variational and diffusion quantum Monte Carlo calculations at nonzero wave vectors: Theory and application to diamond-structure germanium. *Phys. Rev. B*, 51:10591–10600, 1994.
- [53] R. J. Needs, M. D. Towler, N. D. Drummond, and P. L. Rios. *CASINO version 2.3 User Manual*. University of Cambridge, 2008.
- [54] A. Aspuru-Guzik, R. Salomon-Ferrer, B. Austin, R. Perusquia-Flores, M. A. Griffin, R. A. Olivia, D. Skinner, D. Domin, and W. A. Lester. Zori 1.0: A parallel quantum Monte Carlo electronic structure package. *J. Comput. Chem.*, 26:856–862, 2005.
- [55] D. M. Ceperley and L. Mitas. Quantum Monte Carlo methods in chemistry. *Adv. Chem. Phys.*, 93:1–0, 1996.
- [56] D. M. Amow, M. H. Kalos, M. A. Lee, and K. E. Schmidt. Green’s function Monte Carlo for few fermion problems. *J. Chem. Phys.*, 77:5562–0000, 1982.
- [57] D. M. Ceperley and B. J. Alder. Ground state of the electron gas by a stochastic method. *Phys. Rev. Lett.*, 45:566–569, 1980.
- [58] D. M. Ceperley and B. J. Alder. Quantum Monte Carlo for molecules: Green’s function and nodal release. *J. Chem. Phys.*, 81:5833–4844, 1984.
- [59] M. Caffarel and D. M. Ceperley. A bayesian analysis of Green’s function Monte Carlo correlation functions. *J. Chem. Phys.*, 97:8415–8423, 1992.
- [60] Y. Kwon, D. M. Ceperley, and R. M. Martin. Quantum Monte Carlo calculation of the fermi liquid parameters in the two-dimensional electron gas. *Phys. Rev. B*, 50:1684–1694, 1994.
- [61] Y. Kwon, D. M. Ceperley, and R. M. Martin. Transient-estimate Monte Carlo in the two-dimensional electron gas. *Phys. Rev. B*, 53:7376–7382, 1996.
- [62] B. Chen and J. B. Anderson. A simplified released-node quantum Monte Carlo calculation of the ground state of LiH. *J. Chem. Phys.*, 102:4491–4494, 1995.
- [63] J. B. Anderson, C. A. Traynor, and B. M. Boghosian. Quantum chemistry by random walk: Exact treatment of many-electron systems. *J. Chem. Phys.*, 95:7418–7425, 1991.
- [64] D. L. Diedrich and J. B. Anderson. An Accurate quantum Monte Carlo calculation of the barrier height for the reaction $H + H_2 \rightarrow H_2 + H$. *Science*, 258:786–788, 1992.
- [65] R. Bianchi, D. Bressanini, P. Cremaschi, and G. Morosi. Antisymmetry in quantum Monte Carlo methods. *Comput. Phys. Commun.*, 74:153–163, 1993.
- [66] Z. Liu, S. Zhang, and M. H. Kalos. Model fermion Monte Carlo method with antithetical pairs. *Phys. Rev. E*, 50:3220–3229, 1994.
- [67] M. H. Kalos and F. Pederiva. Exact Monte Carlo method for continuum fermion systems. *Phys. Rev. Lett.*, 85:3547–3551, 2000.
- [68] F. Luczak, F. Brosens, J. T. Devreese, and L. F. Lemmens. Many-body diffusion algorithm for interacting harmonic fermions. *Phys. Rev. E*, 57:2411–2418, 1998.
- [69] D. M. Ceperley. Fermion nodes. *J. Stat. Phys.*, 63:1237–1266, 1991.

- [70] R. Bianchi, D. Bressanini, P. Cremaschi, and G. Morosi. Antisymmetry in quantum Monte Carlo method with A -function technique: H_2 b $^3\Sigma_u^+$, H_2 c $^3\Pi_u$, He 1 ^3S . *J. Chem. Phys.*, 98:7204–7209, 1993.
- [71] Y. Mishchenko. Remedy for the fermion sign problem in the diffusion Monte Carlo method for few fermions with antisymmetric diffusion process. *Phys. Rev. E*, 73:026706–10, 2006.
- [72] A. J. W. Thom and A. Alavi. A combinatorial approach to the electron correlation problem. *J. Chem. Phys.*, 123:204106–13, 2005.
- [73] S. B. Fahy and D. R. Hamann. Positive-projection Monte Carlo simulation: A new variational approach to strongly interacting fermion systems. *Phys. Rev. Lett.*, 65:3437–3440, 1990.
- [74] P.L. Silvestrelli, S. Baroni, and R. Car. Auxiliary-field quantum Monte Carlo calculations for systems with long-range repulsive interactions. *Phys. Rev. Lett.*, 71:1148–1151, 1993.
- [75] F. A. Reboredo, R. Q. Hood, and P. R. C. Kent. Self-healing diffusion quantum Monte Carlo algorithms: Direct reduction of the fermion sign error in electronic structure calculations. *Phys. Rev. B*, 79:195117–15, 2009.
- [76] J. C. Slater. Note on the space part of anti-symmetric wave functions in the many-electron problem. *Int. J. Quantum Chem.*, 4:561–570, 1970.
- [77] J. B. Anderson and B. H. Freihaut. Quantum chemistry by random walk: Method of successive corrections. *J. Comput. Phys.*, 31:425–437, 1979.
- [78] J. B. Anderson. Quantum chemistry by random walk: Higher accuracy. *J. Chem. Phys.*, 73:3897–3899, 1980.
- [79] J. B. Anderson. Quantum monte carlo: Direct calculation of corrections to trial wave functions and their energies. *J. Chem. Phys.*, 112:9699–9702, 2000.
- [80] N. Dugan, I. Kanik, and S. Erkoc. Wavefunction correction scheme for non fixed-node diffusion Monte Carlo. (submitted).
- [81] A. Emmanouilidou, T. Schneider, and J.-M. Rost. Quasiclassical double photoionization from the $2^{1,3}\text{S}$ states of helium including shakeoff. *J. Phys. B: At. Mol. Opt. Phys.*, 36:2717–2724, 2003.
- [82] D. H. Bailey and A. M. Frolov. Universal variational expansion for high-precision bound-state calculations in three-body systems. applications to weakly bound, adiabatic and two-shell cluster systems. *J. Phys. B: At. Mol. Opt. Phys.*, 35:4287–4298, 2002.

APPENDIX A

PROOF OF THE VARIATIONAL PRINCIPLE

The variational principle which states that the expectation value of an observable \hat{O} , represented by a linear and Hermitian operator, is larger than or equal to the ground state eigenvalue a_0 :

$$\langle \hat{O} \rangle = \frac{\langle \Psi(\mathbf{x}) | \hat{O} | \Psi(\mathbf{x}) \rangle}{\langle \Psi(\mathbf{x}) | \Psi(\mathbf{x}) \rangle} \geq a_0 , \quad (\text{A.1})$$

can be proven using the eigenfunction decomposition of the arbitrary state $\Psi(\mathbf{x})$ as:

$$\Psi(\mathbf{x}) = \sum_i c_i f_i(\mathbf{x}) , \quad (\text{A.2})$$

where $f_i(\mathbf{x})$ are the orthonormal eigenfunctions of \hat{O} and c_i are the overlap coefficients defined as:

$$c_i = \langle f_i(\mathbf{x}) | \Psi(\mathbf{x}) \rangle . \quad (\text{A.3})$$

Substituting the $\Psi(\mathbf{x})$ expression given in Eq. A.2 in Eq. A.1 gives:

$$\langle \hat{O} \rangle = \frac{\langle \sum_i c_i f_i(\mathbf{x}) | \hat{O} | \sum_j c_j f_j(\mathbf{x}) \rangle}{\langle \sum_i c_i f_i(\mathbf{x}) | \sum_j c_j f_j(\mathbf{x}) \rangle} . \quad (\text{A.4})$$

Using the eigenvalue equation $\hat{O} f_i(\mathbf{x}) = a_i f_i(\mathbf{x})$ and the linearity, Eq. A.4 becomes:

$$\langle \hat{O} \rangle = \frac{\langle \sum_i c_i f_i(\mathbf{x}) | \sum_j c_j a_j f_j(\mathbf{x}) \rangle}{\langle \sum_i c_i f_i(\mathbf{x}) | \sum_j c_j f_j(\mathbf{x}) \rangle} . \quad (\text{A.5})$$

The orthonormality of the eigenfunctions is used to convert the above expression into the simple form:

$$\langle \hat{O} \rangle = \frac{\sum_{i,j} c_i^* c_j a_j \delta_{ij}}{\sum_{i,j} c_i^* c_j \delta_{ij}} = \frac{\sum_i c_i^* c_i a_i}{\sum_i c_i^* c_i} = \frac{\sum_i |c_i|^2 a_i}{\sum_i |c_i|^2} . \quad (\text{A.6})$$

Using the fact that the eigenvalues a_i are greater than or equal to the ground state eigenvalue a_0 , the above equality is converted to an inequality:

$$\langle \hat{O} \rangle \geq \frac{\sum_i |c_i|^2 a_0}{\sum_i |c_i|^2} . \quad (\text{A.7})$$

The constant a_0 can be taken out of the sum, yielding:

$$\langle \hat{O} \rangle \geq \frac{a_0 \sum_i |c_i|^2}{\sum_i |c_i|^2} = a_0 , \quad (\text{A.8})$$

which proves Eq. A.1.

CURRICULUM VITAE

Surname : Dugan

Name : Nazım

Nationality : T.C.

Email : ndugan@metu.edu.tr

Phone : +90 312 210 4307

EDUCATION

Ph.D in Physics, 2006 : 2010, Middle East Technical University

Supervisor: Sakir Erkoc

Thesis Title: Quantum Monte Carlo Methods for Fermionic Systems: Beyond the Fixed-Node Approximation.

MS in Physics, 2005 : 2006, Middle East Technical University

Supervisor: Sakir Erkoc

Thesis Title: Structural Properties of Homonuclear and Heteronuclear Atomic Clusters: Monte Carlo Simulation Study

Ph.D Program in Physics, 2002 : 2004, University of New Hampshire (not completed)

BSc in Physics, 1997 : 2002, Boğaziçi University

EMPLOYMENT

2007 : ongoing, Middle East Technical University

Assistantship in Physics Department, Computer coordinator of the department

2006 : 2007, Middle East Technical University

Teaching Assistantship

2002 : 2004, University of New Hampshire

Teaching Assistantship

Research Assistantship in Computational Space Science Group

2002, Boğaziçi University

Student Assistantship in Physics Department

PUBLICATIONS

N. Dugan, I. Kanik, S. Erkoc, *Wavefunction correction scheme for non fixed-node diffusion Monte Carlo*, arXiv: comp-ph 09123401 (submitted)

N. Dugan, S. Erkoc, *Genetic Algorithms in Application to the Geometry Optimization of Nanoparticles*, Algorithms 2, 410 (2009) (Invited review)

N. Dugan, S. Erkoc, *Genetic Algorithm Application to the Structural Properties of Si-Ge Mixed Clusters*, Materials and Manufacturing Processes 24, 250 (2009)

N Dugan, S. Erkoc, *Genetic algorithm-Monte Carlo hybrid method for geometry optimization of atomic clusters*, Computational Materials Science 45, 127 (2009)

N. Dugan, S. Erkoc, *Stability analysis of graphene nanoribbons by molecular dynamics simulations*, Phys. Stat. Sol. (b) 245, 695 (2008)

N. Dugan, S. Erkoc, *Structural properties of lithium clusters: A Monte Carlo application*, J. Comput. Meth. Sci. Eng. 7, 409 (2007)

N. Dugan, S. Erkoc, *Monte Carlo geometry optimization of Si_n ($n \leq 71$) clusters*, J. Comput. Meth. Sci. Eng. 7, 233 (2007)

N. Dugan, S. Erkoc, *Geometry Optimization of Zn_nCd_m and $(AlTiNi)_n$ Clusters by the Modified Diffusion Monte Carlo Method*, Comput. Lett. 2, 221 (2006)

N. Dugan, S. Erkoc, *Structural Properties of Copper Nanoparticles: Modified Diffusion Monte Carlo Simulations*, Int. J. Mod. Phys. C 17, 1171 (2006)

ATTENDED CONFERENCES AND SUMMER SCHOOLS

13th International Congress on Quantum Chemistry, Helsinki Finland, 2009

Poster: Wavefunction Shift Technique for Exact Diffusion Monte Carlo Computations

14th International Workshop on Computational Physics and Materials Science, Trieste Italy, 2009, Poster: Shifted Wavefunction Diffusion Monte Carlo for Fermions

Quantum Monte Carlo and the Casino Program (Summer School), Vallico Sotto Italy, 2008, Student Talk: Fermion Sign Problem in Diffusion Monte Carlo

NanoTR III, Bilkent University Ankara Turkey, 2007, Talk: Genetic algorithm - Monte Carlo hybrid method for finding stable geometries of atomic clusters

E-MRS Fall Meeting, Warsaw Poland, 2007, Talk: Genetic algorithm-Monte Carlo hybrid method for geometry optimization of atomic clusters

NANOMAT, Antalya Turkey, 2006 Poster: Application of Diffusion Monte Carlo Method to Geometry Optimization of Atomic Nanoparticles.

NanoTR II, METU Ankara Turkey, 2006 Poster: Structural Properties of Copper Nanoparticles